



Scientific Report 10-06

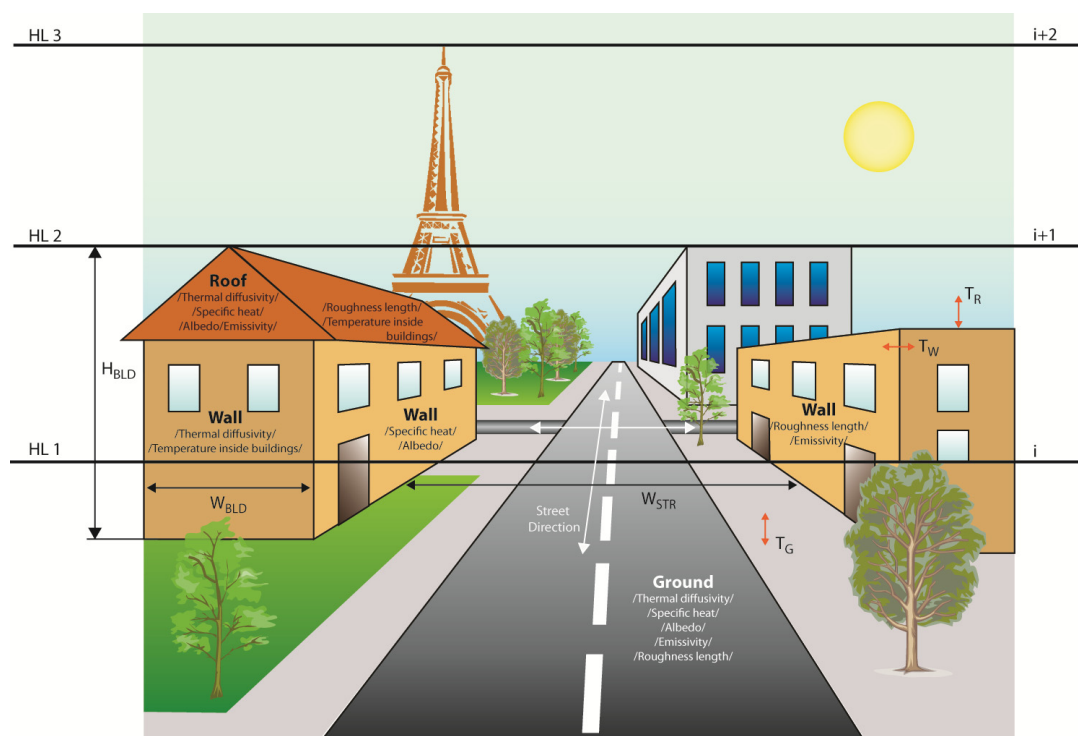
Environmental Modelling in Metropolitan Areas

*Alexander Mahura¹, Roman Nuterman^{1,2}, Iratxe Gonzalez-Aparicio^{1,3},
Claus Petersen¹, Alexander Baklanov¹*

¹ Research Department, Danish Meteorological Institute, DMI, Lyngbyvej 100, DK-2100 Copenhagen Ø, Denmark

² Tomsk State University, TSU, Lenin Avenue 36, 634050, Tomsk, Russia

³ Environment Unit, LABEIN, Tecnalia, Derio, Spain



Colophon

Serial title:

Scientific Report **10-06**

Title:

Environmental Modelling in Metropolitan Areas

Subtitle:

Author(s):

Alexander Mahura, Roman Nuterman, Iratxe Gonzalez-Aparicio,
Claus Petersen, Alexander Baklanov

Other contributors:

Responsible institution:

Danish Meteorological Institute

Language:

English

Keywords:

Building effect parameterization (BEP), urban scale modeling, land surface scheme ISBA, HIRLAM, ...

Url:

www.dmi.dk/dmi/sr10-06.pdf

Digital ISBN:

978-87-7478-606-1 (on-line)

ISSN:

1399-1949 (on-line)

Version:

-

Website:

www.dmi.dk

Copyright:

Danish Meteorological Institute

Application and publication of data and text is allowed with proper reference and acknowledgment



Content:

1. Introduction.....	5
2. Methodology.....	6
2.1. Numerical Weather Prediction and Environmental Modeling.....	6
2.1.1. HIRLAM.....	6
2.1.2. Enviro-HIRLAM.....	7
2.1.3. Nesting of Models / Downscaling.....	7
2.2. Building Effects Parameterization (BEP) Module.....	9
2.2.1. Background Description.....	9
2.2.2. Urban Module Structure and Implementation.....	10
2.2.3. Urban Class in Different Modelling Domains.....	12
2.2.4. Urban Class at Different Resolutions.....	13
2.2.5. Characteristics of Urban Districts.....	15
2.3. Meteorology Analysis and Selection of Specific Cases/Dates.....	19
2.4. Downscaling Meteorology.....	21
2.5. Downscaling Chemistry.....	22
3. Results and Discussions.....	24
3.1. Air Temperature at 2m.....	24
3.2. Relative Humidity at 2m.....	27
3.3. Boundary Layer Height.....	29
3.4. Wind Speed at 10m.....	30
3.5. Surface Temperature.....	32
3.6. Total Cloud Cover.....	33
3.7. Ozone Concentration.....	34
4. Conclusions.....	38
Acknowledgments.....	39
References.....	39
Appendix A1: Analysis of vertical sounding for Trappes station.....	41
Appendix A2: Case study: 3-4 Jul 2009 – Meteorological situation.....	43
Appendix A3: List of chemical species used in the chemical mechanism.....	44

Abstract

The influence of the Paris Metropolitan Area (PMA, France) on formation and development of meteorological and chemical patterns fields was investigated applying the downscaling (15-5-2.5 km horizontal resolution) for the on-line integrated meteorology-chemistry/aerosols Enviro-HIRLAM (Environment – High Resolution Limited Area Model) runs. The runs were performed in two modes: control vs. modified (with Building Effect Parameterization module and varying Anthropogenic Heat Flux included) for the MEGAPOLI Paris Measurement Campaign. Changes in meteorological and chemical patterns were evaluated on a diurnal cycle due to inclusion of urban effects into the model. It was shown that urban effects can be of considerable importance over the large metropolitan areas such as Paris. Changes were identified for both meteorological parameters as well as for concentration of chemical species. Inclusion of urban effects does not substantially increase the computational time. Hence, such modifications are suitable for purposes of operational high resolution numerical weather prediction. The approaches applied as well as results obtained in this study will be used for reporting in the FP7 EU MEGAPOLI project (<http://megapoli.info>) as well as for lecturing material and practical exercises for the YSSS-2011 (Jul 2011, Odessa, Ukraine; <http://www.ysss.osenu.org.ua>).



1. Introduction

In recent decades, continuously increased resolution and improved land-use classifications for urban areas, based on existing land databases such as ECOCLIMAP, PELCOM, GLCC, and others lead to further development of urban parameterization useful for Numerical Weather Prediction (NWP) systems. Improved land-use classifications and models for computing in urban areas for NWP systems are based on the following. First, the increased resolution surface databases (such as CORINE, DHM, etc.) for refined calculation of the roughness length, momentum, heat, and moisture fluxes in operational NWP models became available. Second, different modified algorithms for estimation of roughness parameters within urban areas based on morphologic methods have been developed and tested. For that different databases on urban characteristics were analyzed for mapping morphology and aerodynamic parameters which are characteristic for urban areas, and specifically, for different types of urban districts. Third, experimental studies of urban roughness non-homogeneity effects on the urban boundary layer development were carried out, and these results were used for model verifications. Additionally, within the urban areas, the urban heat fluxes, e.g., via heat/ energy production/ using in the city, heat storage capacity, etc., are important to be considered in the surface heat flux calculation in NWP models run over the urban areas.

There is a variety of modules/ schemes/ parameterizations used for improvement of simulations within the urban areas. These can be implemented into NWP models or their post-processors. For example, corrections of the surface roughness (and displacement height) for urban areas (e.g., following to *Bottema, 1997; Grimmond and Oke, 1999*) and heat fluxes (adding the additional urban heat flux., e.g., via heat/ energy production/ using in the city, heat storage capacity and albedo change) can be done within the existing non-urban physical parameterizations of the surface layer in the NWP model having a higher resolution and improved land-use classification.

Such corrections were implemented in the NWP DMI-HIRLAM model; and the model performance was estimated for specific case studies under different meteorological conditions as well as long-term simulations/ verification (*Mahura et al., 2004; Mahura et al., 2005b; Mahura et al., 2006*). The domain studied included the Copenhagen metropolitan area of Denmark. Specific dates and NWP operational meteorological data were used.

The urban surface exchange parameterization, so-called the Building Effects Parametrization (BEP; *Martilli et al., 2002*) was also tested for the DMI-HIRLAM model by *Mahura et al. (2008)* for the same metropolitan area. An evaluation of NWP model's urbanization was done for period from 1 July till 31 August 2004, and verification results were summarized for forecasted diurnal cycle of wind velocity, air temperature and relative humidity fields for all stations and selected urban stations in the Copenhagen metropolitan and surroundings.

Moreover, the Soil Model for Sub-Meso scales – Urban version (SM2-U; *Dupont, 2001; Mestayer et al., 2004; Dupont & Mestayer, 2006; Dupont et al., 2006*) was tested for the Copenhagen metropolitan area (*Mahura et al., 2005a*). The large eddy simulations employing the NWP SUBMESO model with the urban soil layer model SM2-U were performed and monthly and diurnal cycle variability were studied for the net radiation, sensible and storage heat fluxes, surface's temperatures, and others. These were evaluated for selected urban vs. non-urban related types of covers/surfaces and urban districts such as city center, high buildings, industrial, and residential. Results showed strong effects of urban features on temporal and spatial variability. They are useful and applicable for verification of numerical weather prediction models and development of urban canopy parameterizations.

The main goal of this study is to estimate an influence of the Paris metropolitan area (France) on formation of the 3D meteorological variables' and chemical species' fields within the metropolitan area itself and surroundings. For that, at first, the Enviro-HIRLAM model (Korsholm *et al.*, 2008; Korsholm, 2009) was modified by implementation of the urban module (BEP; Martilli *et al.*, 2002). The period considered included two FP7 EC MEGAPOLI (<http://megapoli.dmi.dk>) Paris Summer (1-31 Jul 2009) and Winter (15 Jan – 14 Feb 2010) measurement campaigns carried within the Paris metropolitan area and surroundings and included ground, mobile, and airborne types of observations. The model was run with increasing (from a crude to a fine) of spatial horizontal resolution and down-scaling. The run followed in two modes: 1) without urban module (control run), and 2) with urban module (BEP run). The generated output was evaluated for changes in meteorological (air temperature and relative humidity at 2 m, surface temperature, cloud cover, wind at 10 m, boundary layer height) and chemical (on example of ozone) patterns on a diurnal cycle due to inclusion of urban effects into the model. Various specific dates during mentioned periods were simulated and which were characterized by different types of meteorological and air pollution levels - low, typical, and high wind conditions, high precipitation, and high pollution levels dates.

2. Methodology

2.1. Numerical Weather Prediction and Environmental Modeling

2.1.1. HIRLAM

The Numerical Weather Prediction (NWP) DMI - High Resolution Limited Area Model (DMI-HIRLAM) is used for operational forecasting of weather conditions. At present, output from several nested versions of DMI-HIRLAM model (from original HIRLAM (<http://hirlam.org>; Unden *et al.*, 2002), then adapted and refined version) with different resolutions is applied: (Figure 2.1.1.1):

- T15 – 15 x 15 km, 40 vertical layers;
- M09 – 9 x 9 km, 40 vertical layers;
- K05 – 5 x 5 km, 40 vertical layers;
- S05 – 5 x 5 km, 40 vertical layers;
- S03 – 3 x 3 km, 40 vertical layers.

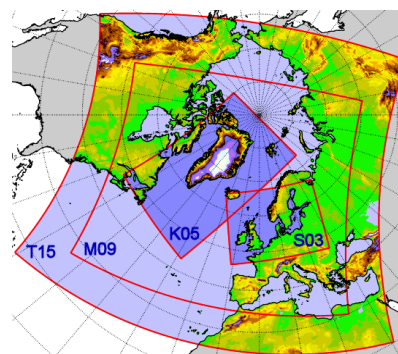


Figure 2.1.1.1: NWP DMI-HIRLAM operational and research modelling domains.

The current operational DMI forecasting modelling system (Yang *et al.*, 2005) includes the pre-processing, climate file generation, data assimilation, initialization, forecasting, post-processing, and verification. It includes also a digital filtering initialization, semi-Lagrangian advection scheme, and a set of physical parameterizations such as Savijaervi radiation, STRACO condensation, CBR turbulence scheme, and ISBA scheme. The lateral boundary conditions are received every 6 hour from ECMWF. The system is running on the DMI CRAY-XT5 supercomputer and produced model output files after forecasts is finished, will be archived on a mass storage system.

The operationally produced 3D meteorological fields output can be used as input data for different applications, for example, as input for atmospheric chemical transport (ACT) models, pollen forecasting, chemical weather forecasting, emergency response, and other tasks. Moreover,

afterwards archived datasets, including re-analysed fields, can be used for analysis of specific meteorological cases, climatological runs, etc.

At present, output from several nested versions of the DMI-HIRLAM as shown in Figure 2.1.1.1 (originally developed from HIRLAM (<http://hirlam.org>) model and further adapted and refined for Denmark) is generated daily with a possibility of short- and long-term storage of simulated 3D meteorological fields at surface and model levels. Note that the DMI-HIRLAM–S03 and –S05 models have very similar geographical boundaries of the modeling domains. Moreover, there are domains covering Denmark with higher resolution (–U01/ –I01: 1.4 x 1.4 km, 40 vertical layers) and these are used as an experimental urbanized version.

2.1.2. Enviro-HIRLAM

The Enviro-HIRLAM (Environment - High Resolution Limited Area Model) is an on-line coupled NWP and ACT model for research and forecasting of both meteorological and chemical weather. The integrated modelling system is developed by DMI and other collaborators (*Chenevez et al., 2004; Baklanov et al., 2008; Korsholm et al., 2008, Korsholm, 2009*). At the current stage the Enviro-HIRLAM model is used as a baseline system for the HIRLAM Chemical Branch (<https://hirlam.org/trac/wiki>), and additionally to the HIRLAM community the following groups join the development team: University of Copenhagen (Denmark), Tartu University (Estonia), Russian State Hydro-Meteorological University, Tomsk State University, Odessa State Environmental University (Ukraine), etc.

Enviro-HIRLAM includes two-way feedbacks between air pollutants and meteorological processes. Atmospheric chemical transport equations are implemented inside the meteorological corner on each time step (*Chenevez et al., 2004*). To make the model suitable for CWF in urban areas, where most of population is concentrated, the meteorological part is improved by implementation of urban sublayer modules and parameterisations. The aerosol module in Enviro-HIRLAM comprises two parts: (i) a thermodynamic equilibrium model (NWP-Chem-Liquid) and (ii) the aerosol dynamics modele (*Gross and Baklanov, 2004*) based on the modal approach. Parameterisations of the aerosol feedback mechanisms in the Enviro-HIRLAM model are described in *Korsholm et al. (2008; 2009)*. Several chemical mechanisms could be chosen depending on the specific tasks: well-known RADM2 and RACM or new-developed economical NWP-Chem (*Korsholm et al., 2008*) mechanism. Validation and sensitivity tests of the on-line versus off-line integrated versions of Enviro-HIRLAM showed that the on-line coupling improved the results (*Korsholm et al., 2008*). Different parts of Enviro-HIRLAM were evaluated versus the ETEX-1 experiment, Chernobyl accident and Paris study datasets and showed that the model performs satisfactorily (*Korsholm, 2009*).

2.1.3. Nesting of Models / Downscaling

In our study, the nesting from Enviro-HIRLAM–P15 to –P05 and to –P01 (with horizontal resolutions of 15, 5, and 2.5 km, respectively) has been done for both the meteorological variables' and chemical species' fields. The downscaling chain is shown in Figure 2.1.3.1. In order to run the chain, the initial and boundary conditions are required, and these are taken from the ECMWF. In general, a set of models (as ensemble) vs. one single mode can be run. Here, the Enviro-HIRLAM model runs subsequently at 3 different resolutions serving input for a higher resolution model run from outer to inner model. The urbanization is implemented only at the finest resolution run. The produced output at all runs can serve as input for possible assessment studies and decision making process by authorities at different level.

The nested domains with setup parameters are shown in Figure 2.1.3.2. The P01 domain was selected in order to focus on evaluation of the urban areas effects on a formation of meteorological and chemical species fields taking into account changing atmospheric composition. The modeling domains are represented in the rotated system of coordinates, where the selected South Pole latitude and longitude are defined. For the domains the south, west, north, and east boundaries are also given in the rotated system of coordinates. Parameters also include the number of grid points along rotated longitude and latitude and number of vertical levels (40 for all domains). The total number of passive boundary points from the borders of modeling domains is the same for all models and equal to 10. The total number of grid cells is equal to 22792, 6660, and 10148 for the P15, P05, and P01 domains, respectively.

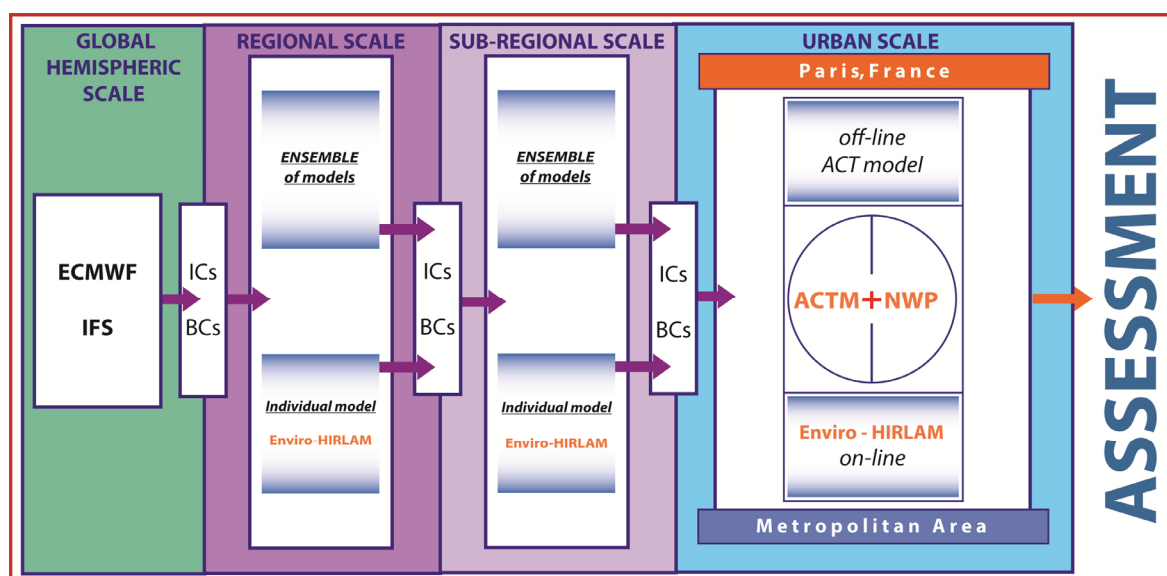


Figure 2.1.3.1: Downscaling chain of the Enviro-HIRLAM model runs at different resolution.

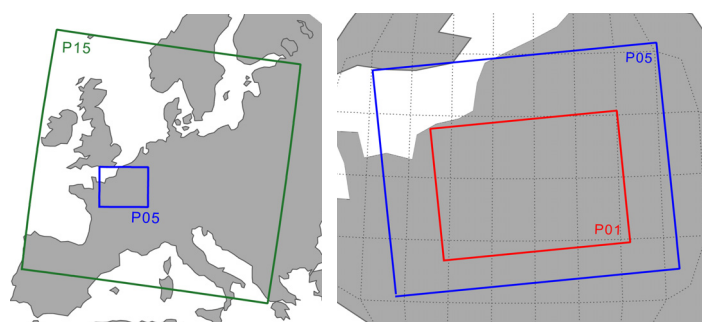


Figure 2.1.3.2: Boundaries of nesting domains of different resolution: P15, P05, and P01; and models' setup parameters.

Resolution	15 km	5 km	2.5 km
Domain	P15	P05	P01
Size			
NLON	154	90	86
NLAT	148	74	118
NLEV	40	40	40
PLON	0	10	10
PLAT	-40	-40	-40
Boundaries			
SOUTH	-9.505	-2.450	-1.950
WEST	-6.505	-6.925	-6.125
NORTH	12.545	1.200	0.175
EAST	16.445	-2.475	-3.200
Grids	22792	6660	10148

The terrain over the finest resolution model domain (P01) is shown in Figure 2.1.3.3. Surroundings of the Paris metropolitan area are ranging in height from 31 to almost 400 m above sea level (asl). The Paris metropolitan area is situated on the Seine River spreading largely on both banks of the river. It is in the center of the so-called "Ile-de-France" region. Paris itself is placed over relatively flat terrain although there are also several surrounding hills up to 130 m asl.

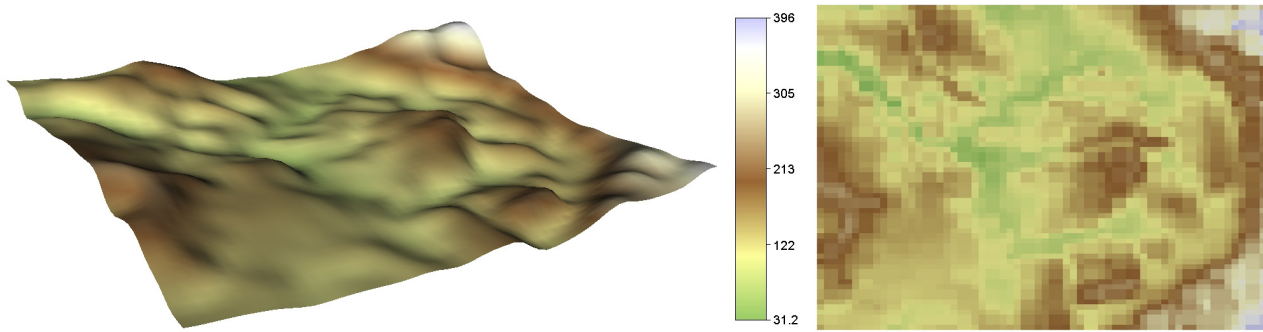


Figure 2.1.3.3: Terrain variability within the P01 modeling domain.

Analysis of test runs showed that different computational time is required to perform the runs at different horizontal resolution and time steps. In particular, runs for the P15, P05, and P01 domains (see Table in Figure 2.1.3.2) required about 1.16, 0.83 and 2.3 hours, respectively (at 240, 120, and 60 sec time step). Run-time sensitivity tests for P01 domain at different time steps of 30 and 90 sec showed that the total CPU time required is about 4.67 and 1.83 hours, correspondingly.

2.2. Building Effects Parameterization (BEP) Module

2.2.1. Background Description

The city in the urban sub-layer parameterisation, so-called the Building Effects Parameterization (BEP) module (Martilli *et al.*, 2002) is represented as multiple streets and buildings of constant widths, but with different heights (see Figure 2.2.1.1). In this case, the urban parameterisation needs as input a set of different parameters for the ground, wall and roof surfaces. In this parameterization the city is given as a combination of several urban classes/ districts. Each class is characterized by an array of buildings of the same width located at the same distance from each other (i.e. canyon width), but with different heights (with a certain probability to have a building with a certain height). To simplify the formulation it is assumed that the length of the street canyons is equal / or larger to the horizontal grid size. The vertical urban structure is defined on a numerical grid.

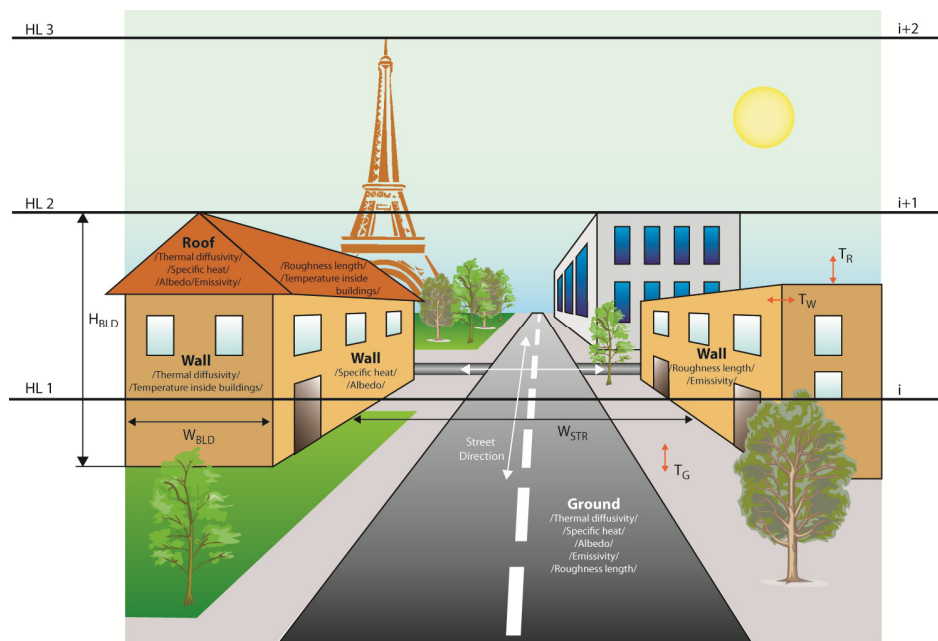


Figure 2.2.1.1: Schematic representation of urban features and numerical grid in the urban module / HL1, HL2 – model levels; H_{BLD} , W_{BLD} – height and width of the buildings; SD, W_{STR} – street direction and width; T_G , T_W , T_R – temperatures of ground, wall and roof surfaces, respectively/.

The used method includes computing of contributions from every type of urban surface (street canyon floor; roofs and walls of buildings) for the momentum, heat and turbulent kinetic energy equation separately as contributions of the vertical surfaces (building walls) as well as horizontal surfaces (street canyon floor and roofs). The mentioned surfaces at each level are calculated using priority defined characteristics of the urban class (street and buildings width and height as well as density of buildings).

The contributions of the horizontal surfaces (canyon floor and roofs) are calculated using the formulation of *Louis (1979)* based on the Monin-Obukhov Similarity Theory (MOST). The exchange of momentum and turbulent kinetic energy on the vertical surfaces (walls) are parameterized as the effect of pressure and drag forces induced by the buildings. The temperature fluxes from the walls are a function of the difference between the air temperature and the wall temperatures. They are parameterized using the formulation of *Clarke (1985)* proposed by *Arnfield & Grimmond (1998)* in their urban energy budget model. To compute the surface temperatures of roofs, walls and canyon floor a heat diffusion equation is solved in several layers in the material (concrete or asphalt) and an energy budget is computed for every surface, where calculation of the radiation takes into account shadowing and radiative trapping effects of the buildings. To compute the wall, street and roof temperatures, a heat diffusion equation is solved in several layers at the interior of the material (asphalt or concrete). This equation is solved for street, roof and for east and west walls at every model level below the roof level.

Since the urban parameterization should be used in a mesoscale model and the numerical grid where the urban fluxes are computed can be different from the grid of the mesoscale model, a procedure of averaging/interpolation is needed to connect the two grids. From mesoscale to urban: the computation of the fluxes induced by the presence of the buildings requires the values of the wind and air temperature as input. A volumetric interpolation of these values from the 'mesoscale' grid (the grid where these values are computed) to the urban grid is performed. From urban to mesoscale: the contribution of the urban areas in the energy equations is the average (interpolation to the grid of the mesoscale model) of the fluxes computed on the urban grid due to the presence of the buildings.

The advantage of the surface heat fluxes calculation is that it takes into account the main characteristics of the urban environment: 1) vertical and horizontal surfaces (wall, canyon floor and roofs); 2) shadowing and radiative trapping effects of the buildings; and 3) anthropogenic heat fluxes through the buildings wall and roof. The Martilli's urban scheme explicitly considers the effects of buildings, roads, and other artificial materials on the urban surface energy budget. This urban module had been tested with a mesoscale model TVM (*Schayes et al, 1996*) and the model is run off-line on a 1D-column. It was also validated using data from the BUBBLE campaign.

2.2.2. Urban Module Structure and Implementation

The urban sub-layer parameterization is composed of the following (see Figure 2.2.2.1). The structure of the NWP model starts generally with an initialization step. Following the initialization, the program compute successively the pressure, the advection and the turbulent viscosity-diffusivity at each time step and cell having urban fraction. The first segment reads, computes, and initializes the urban characteristics during the initialization step of the NWP model. The second segment computes the urban effects for the diffusion-viscosity resolution within the turbulence part of the code.

1st Segment - IC_URBAN

Input: 1) file with urban characteristics; 2) number of horizontal spatial steps in X and Y directions; 3) potential temperature and pressure in each cells at the ground.

Output: 1) initial temperature in each layer of the wall and roof of buildings and canyon floor, 2) urban characteristics, and urban grid resolution.

2nd Segment - URBAN

Input: 1) vertical resolution of meteorological model's grid (the column); 2) time step; 3) wind speed in X and Y directions; 4) potential temperature; 6) air density; 7) atmospheric pressure; 8) solar radiation and zenith angle; 9) urban characteristics initialized and computed in IC_URBAN.

Output: 1) terms for computing the vertical diffusion; 2) average of the road surface temperatures; 3) parameters for computing the turbulent diffusion coefficients and source and sink terms in the TKE equation.

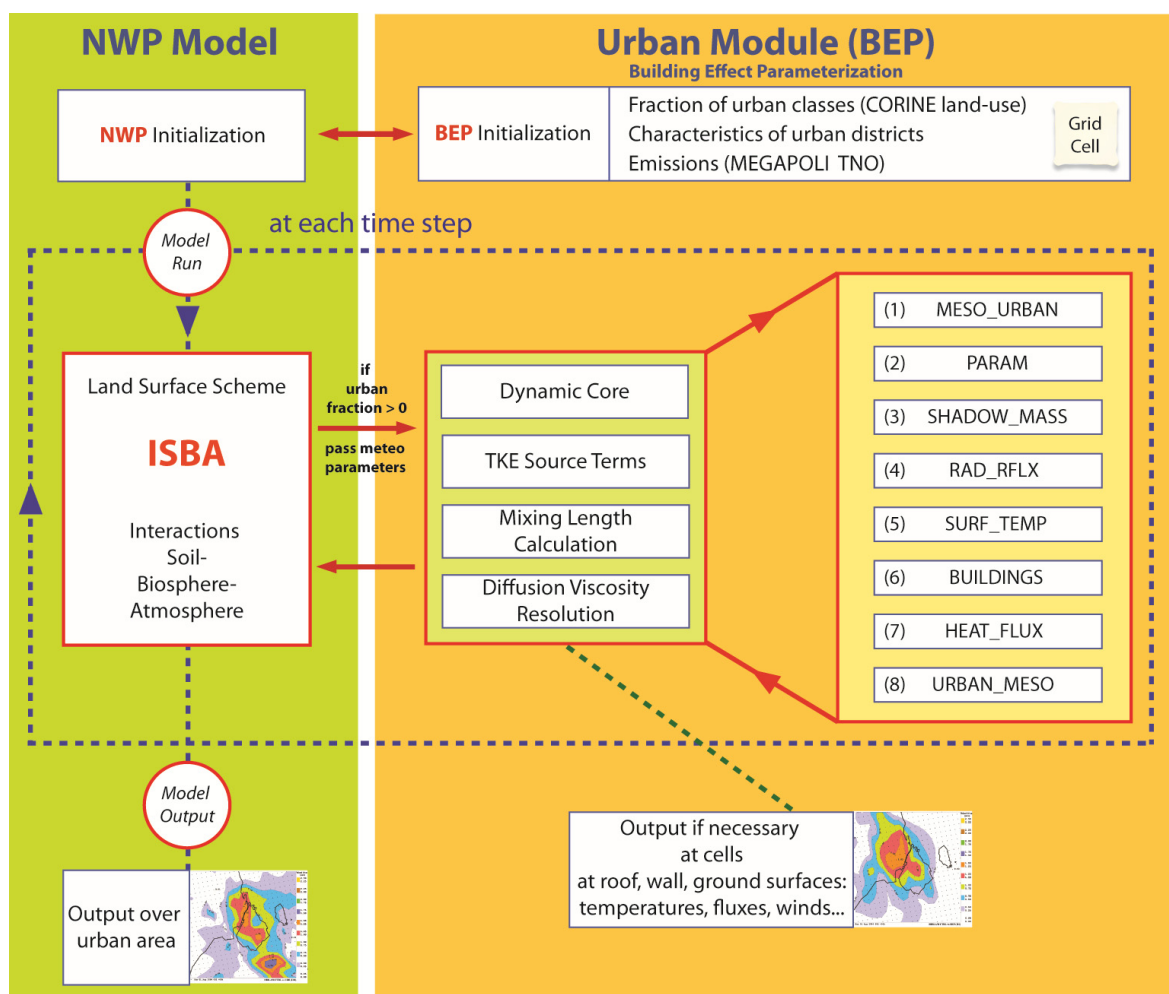


Figure 2.2.2.1: General scheme of the BEP module for the model urbanization with a structure of the subroutine conception.

The URBAN subroutine includes the following (see Figure 2.2.2.1):

- (1) MESO_URBAN: Vertical interpolation of the meso-scale variable (wind speed, temperature, pressure, etc.) to the urban grid;
- (2) PARAM: Parameters (characteristic of materials, albedo, emissivity, etc.) used for computation of heat fluxes;
- (3) SHADOW_MASS: Computing shadow effects and adjustment of short-wave radiation due to the buildings;

- (4) RAD_RFLX: Computing adjustment of long-wave radiation due to the buildings;
- (5) SURF_TEMP: Computing temperature in/on the roof, wall and ground surfaces; and transfer of heat flux from mentioned surfaces to the interior;
- (6) BUILDINGS: Computing new values of $ustar$, $tstar$ for horizontal surfaces; and flux at the ground;
- (7) HEAT_FLUX: Implicit computation of sensible heat fluxes from the wall, roof and ground;
- (8) URBAN_MESO: Averaging and interpolating the surface's impacts on the meso-scale grid.
/this routine is the connection between the urban grid and the meso-grid/.

2.2.3. Urban Class in Different Modelling Domains

Numerical simulations and fields measurements indicate that increasing vegetation cover in urban area can be effective in reducing the surface and air temperatures near the ground. So, for the ISBA scheme the fractions of vegetation relevant tiles (i.e. low vegetation and forest) in grid cells are calculated and included into the monthly climate generation files. The analysis of fractions in grid cells of the P01 domain showed that 38.16% of these cells (i.e. from 10148 cells, in total) have been occupied by forest of different types (i.e. evergreen, deciduous, and mixed), and 41.32% - by low vegetation (i.e. combined of cropland, grass, shrubs, etc.).

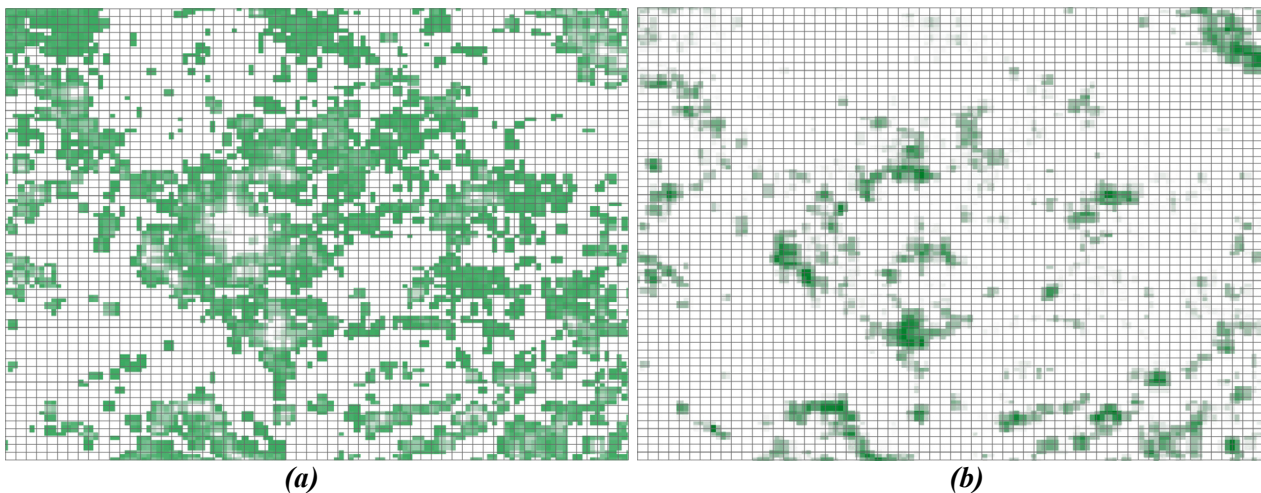


Figure 2.2.3.1: Representation of grid cells with different fractions of the (a) low vegetation and (b) forest tiles in the ISBA scheme of the model (variability within the P01 modeling domain).

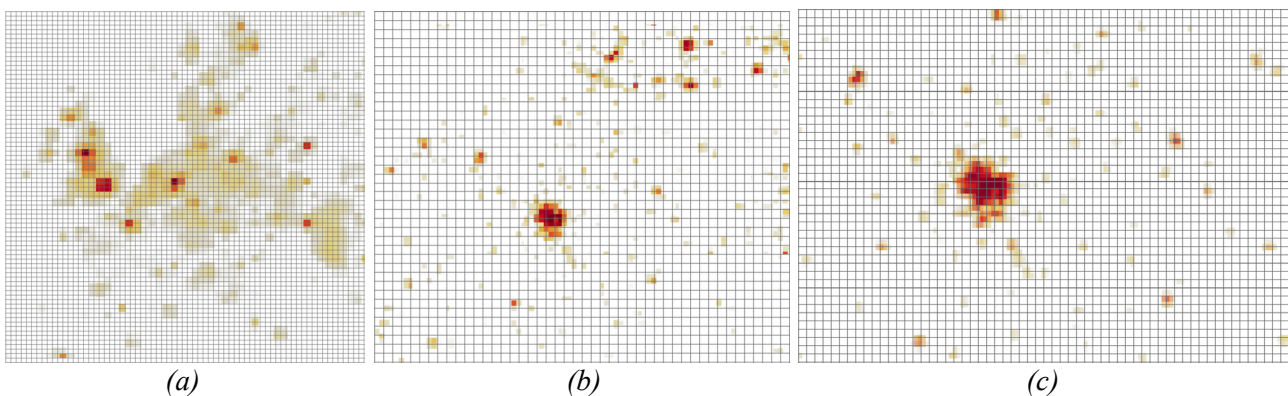


Figure 2.2.3.2: Representation of urban grid cells with different fractions in modeling domains: (a) P15, (b) P05 /grids are plotted at 25 km resolution/, and (c) P01 /grids are plotted at 5 km resolution/.

The presence of urban class within modeling domains is shown in Figure 2.2.3.2. Note, that the current ISBA scheme in HIRLAM is treating the urban class as a tile having bare soil characteristics. Moreover, this class is rare appearing when the 1st and 2nd dominating classes are

selected for the grid cells. The frequency of urban cells in three selected domains is shown in Figure 2.2.3.3, with clearly seen skewed (to the left) type of distribution having largest number of the cells with a smaller fraction of urban class.

A summary is given in Table 2.2.3.1. In general, the number of grid cells (e.g. any grid cell having, at least, non-zero urban fraction) in the modelling domains varies greatly, but the percentage of cells with urban class treated as the 1st and 2nd dominating is larger for the higher resolution domains. Due to size of grid cells, the minimum and maximum fraction of urban class varies as well. It is the largest for the P01 domain (maximum fraction of 1 or 100%; and minimum fraction of 0.019 or about 2%) compared with other lower resolution domains. In particular, the maximum fraction of urban class in cell is less than 0.3 (or 3%) at 15 km resolution, and it is the highest (1 or 100%) at 2.5 km resolution, e.g. by factor of more than 3. More details are shown in section 2.2.4.

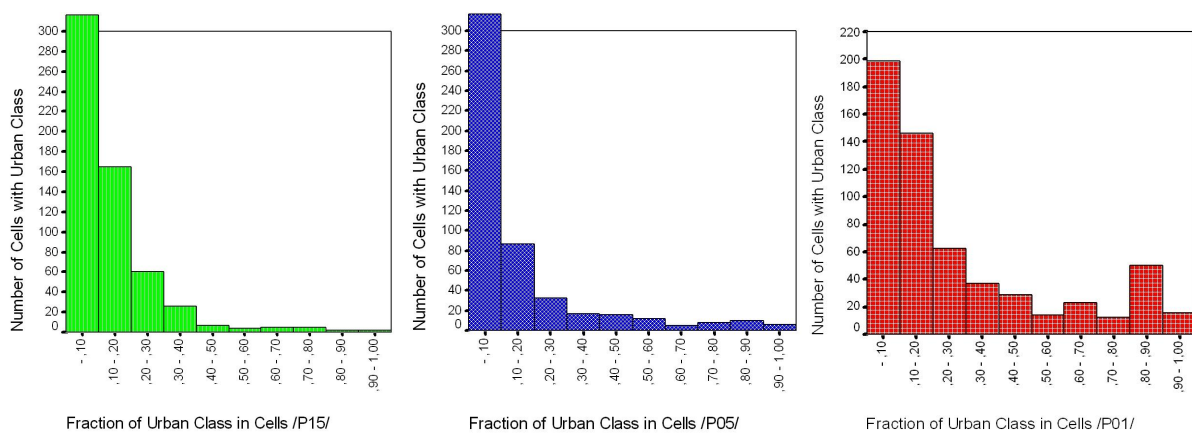


Figure 2.2.3.3: Frequencies of urban cells for different ranges of fractions within the geographical boundaries of the P15, P05, and P01 modeling domains.

Parameters	Domains	P15	P05	P01
Total number of grid cells in domain		22792	6660	10148
% of non-urban cells in domain		80.02	88.89	94.21
Number of cells having a fraction of urban class		4555	740	588
% of cells with urban class treated as 1 st dominating class		0.11	0.77	2.18
% of cells with urban class treated as 2 nd dominating class		2.15	1.64	1.54
Min fraction of urban class in cell		0.0005	0.0038	0,0190
Max fraction of urban class in cell		0.271	0.914	1.000

Table 2.2.3.1: Summary statistics on urban grid cells for three (P15, P05, P01) selected modeling domains.

2.2.4. Urban Class at Different Resolutions

A summary statistics (for all three model domains) for fractions of urban grid cells within the boundaries of the P01 domain is shown in Table 2.2.4.1. As seen, there are 122 cells (from P15) within P01 domain having mean urban fraction of about 0.04 (or 4%) compared with 588 cells within P01 itself having mean urban fraction of about 0.28 (or 28%). It is almost 7 times larger. The minimum urban fraction is about 0.2 (or 2%) within a grid cell of the P01 domain, and it is almost negligible for both P15 and P05. Moreover, as seen the maximum fraction for P15 is only about 0.22 (or 22%), although for P05 and P01 it reaches 0.9 and 1 (or 90 and 100%), respectively. Figure 2.2.4.2 shows frequencies of urban cells distribution for different ranges of fractions within the geographical boundaries of the P01 domain for the same selected modeling domains.

These brief analyses allow assuming that presence (e.g. larger number and larger fraction) of urban grid cells within boundaries of the P01 domain can lead to better representation of the metropolitan/urban area for the modelling purposes, e.g. more urban effects might be accounted.

Domains	P15	P05	P01
Parameters			
<i>Number of urban grid cells</i>	122	301	588
<i>Mean fraction</i>	0,038	0,140	0,281
<i>Median</i>	0,010	0,044	0,166
<i>Std. Deviation</i>	0,117	0,230	0,295
<i>Variance</i>	0,014	0,053	0,087
<i>Skewness</i>	5,505	2,410	1,322
<i>Kurtosis</i>	33,121	5,104	0,489
<i>Minimum</i>	0,0005	0,0038	0,0190
<i>Maximum</i>	0,216	0,896	1,000
<i>Sum</i>	4,687	42,168	165,276

Table 2.2.4.1: Summary statistics for fractions of urban grid cells within the geographical boundaries of the P01 domain for three selected modeling domains.

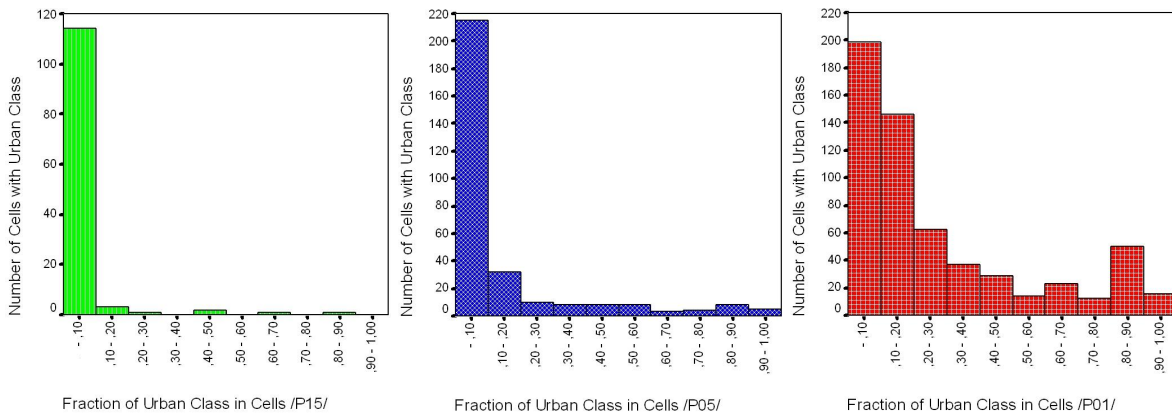


Figure 2.2.4.2: Frequencies of urban cells for different ranges of fractions within the geographical boundaries of the P01 domain for 3 selected modeling domains.

Parameters	Count	Median	Mean	Std Dev	Variance	Sum
Models	<i>Urban fraction in grid cell ≥ 0.25</i>					
P01	208	3,47	3,82	1,66	2,77	794
P05	49	12,98	14,96	6,19	38,35	733
P15	4	129,39	138,31	50,74	2574,31	553
	<i>Urban fraction in grid cell ≥ 0.50</i>					
P01	120	5,21	5,02	1,10	1,219	602
P05	28	19,69	19,25	4,59	21,11	539
P15	2	179,18	179,18	31,63	1000,19	358
	<i>Urban fraction in grid cell ≥ 0.75</i>					
P01	72	6,08	5,83	0,50	0,25	420
P05	15	23,34	23,04	1,86	3,47	346
P15	1	201,54	201,54	.	.	202

Table 2.2.4.1 : Summary statistics for areas (km²) of urban grid cells with different fractions within the geographical boundaries of the P01 domain for 3 selected modeling domains.

The distribution of areas within the urban grid cells is summarized in Table 2.2.4.1. The area occupied by individual grid cell is roughly 225, 25, and 6.25 km² for the P15, P05, and P01 domains, respectively.

General statistics for urban grid cells with respect to occupied area was obtained. Since previous studies showed that urban effects became visible in urban cells having a fraction of more than 0.25 (25%), the analysis was performed considering a contribution from different fractions of urban type in grid cell. It showed that the total area occupied by urban cells (with different fractions) is higher for P01 compared with others domains. Moreover, the number of urban related cells decreases significantly when cells with higher urban fractions are considered. For example, if urban cells with a fraction of more than 0.75 are considered then the total urban area is more than twice (420 vs. 202 km²) larger for P01 (i.e. at a fine resolution) compared with P15 (i.e. at a crude resolution). A large city or metropolitan area in such a domain will be represented by only one grid cell, and therefore, urban effects have the lowest likelihood to be produced during the model run and such effects will not be visible in the meteorological variables' fields. In general, starting at a fraction of 0.25, the influence of urban territories became visible. In our case the total area occupied by urban cells having such fraction is 794, 733, and 553 km² for the P01, P05, and P15; moreover, such distribution (with respect to horizontal resolution) between models remains relatively similar with increasing fraction's content.

2.2.5. Characteristics of Urban Districts

In our study, classification of urban districts for the Paris metropolitan area was done for grid cells of the P01 modelling domain employing GIS tools and using CORINE dataset. In total, five so-called urban districts were identified for the Paris metropolitan area (see Figure 2.2.5.1). Note, that within the Paris metropolitan area there are several districts which can be treated as the CC type: 13th, 15th and 19th arrondissement of Paris. These include the city center (CC), high buildings district (HBD), industrial commercial district (ICD), residential district (RD), and rural areas (RUR - e.g. grid cells marked in white color - which are not occupied by the urban related districts shown in Figure 2.2.5.1) (e.g. see examples of districts in Figure 2.2.5.2abcde; extracted from Google-Earth).

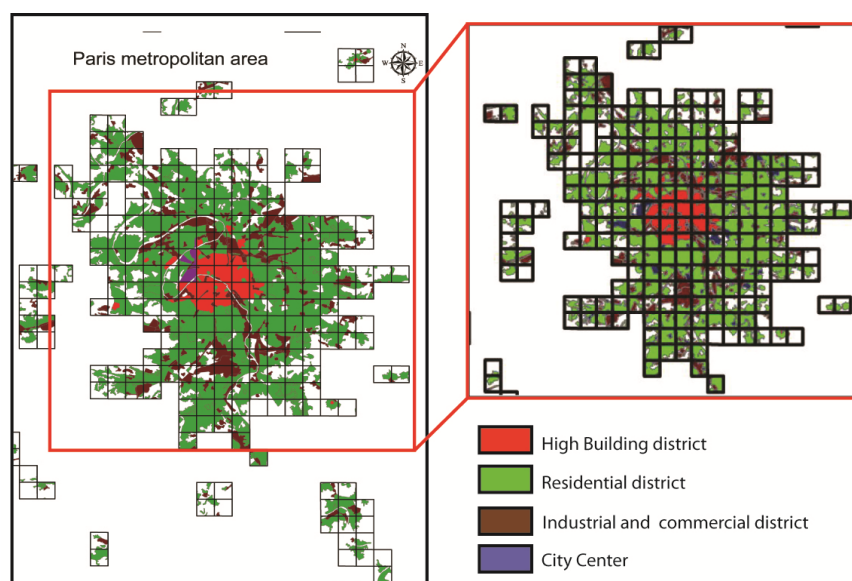


Figure 2.2.5.1: Spatial distribution of urban districts (HBD – high buildings, RD – residential, ICD – industrial commercial, and CC – city center districts) for the Paris metropolitan area within the P01 modelling domain.

Each of these districts is described by a set of specific parameters which includes the thermal diffusivity, specific heat, temperature inside the buildings, albedo, emissivity; roughness length; streets' direction, length, and width; buildings' width and height as well as its probability distribution. Most of these parameters are defined for the ground, wall, and roof surfaces. Summary of districts' parameters (evaluated from different sources; see footnotes) is given in Table 2.2.5.1.

Table 2.2.5.1 : Characteristics of urban districts for the Paris metropolitan area.

Parameters	Type	Units	Urban Districts					Ref
			RD	ICD	CC	HBD	RUR	
Thermal diffusivity	Ground	m ² s ⁻¹	3,60E-07	3,60E-07	3,60E-07	3,60E-07	3,60E-07	1
	Wall	m ² s ⁻¹	5,02E-07	3,32E-06	1,53E-06	1,06E-06	3,71E-07	1
	Roof	m ² s ⁻¹	3,40E-07	5,40E-07	5,40E-07	5,40E-07	3,40E-07	1
Specific heat	Ground	J m ³ K ⁻¹	1,74E+06	1,74E+06	1,74E+06	1,74E+06	1,74E+06	
	Wall	J m ³ K ⁻¹	1,54E+06	1,54E+06	1,54E+06	1,54E+06	1,54E+06	
	Roof	J m ³ K ⁻¹	1,50E+06	1,50E+06	1,50E+06	1,50E+06	1,50E+06	
Temperature inside buildings	Wall	K	291	298	295	293	290	*
	Roof	K	293	300	297	295	292	*
Albedo	Ground		0,2	0,1	0,15	0,2	0,15	2
	Wall		0,2	0,25	0,175	0,2	0,15	2
	Roof		0,2	0,18	0,5	0,2	0,2	2
Emissivity	Ground		0,95	0,95	0,95	0,95	0,28	3
	Wall		0,72	0,9	0,9	0,91	0,72	3
	Roof		0,9	0,78	0,92	0,91	0,9	3
Roughness length	Ground		0.67/1.10	0.61/0.74	0.72/0.98	0.86/1.05	0.67/1.01	4
	Roof		0.67/1.10	0.61/0.74	0.72/0.98	0.86/1.05	0.67/1.01	4
Number of street direction (SD)			2	2	2	2	2	*
Street length	SD 1	m	100000	100000	100000	100000	100000	*
	SD 2	m	100000	100000	100000	100000	100000	*
Street direction	SD 1	radian	0,785	0,785	0,785	0,785	0,785	5
	SD 2	radian	2,355	2,355	2,355	2,355	2,355	5
Street width	SD 1	m	9	10	13	16	7	*
	SD 2	m	9	10	13	16	7	*
Building width	SD 1	m	15	112	30	20	10	*
	SD 2	m	15	112	30	20	10	*
Number of height levels (HL)			2	2	2	2	2	
Building height	HL1	m	5,7	6,09	105,9	21	5,02	6
	HL2	m	5,7	6,09	105,9	21	5,02	6
Probability of building height	HL1		100	75	50	60	100	*
	HL2		0	25	50	40	0	*

1

¹ <http://de.wikipedia.org/wiki/Temperaturleit%C3%A4higkeit> & http://en.wikipedia.org/wiki/Thermal_diffusivity

* own rough estimations

² Derived from Table 1, Albedo Concrete and Other Materials & Figure with albedo

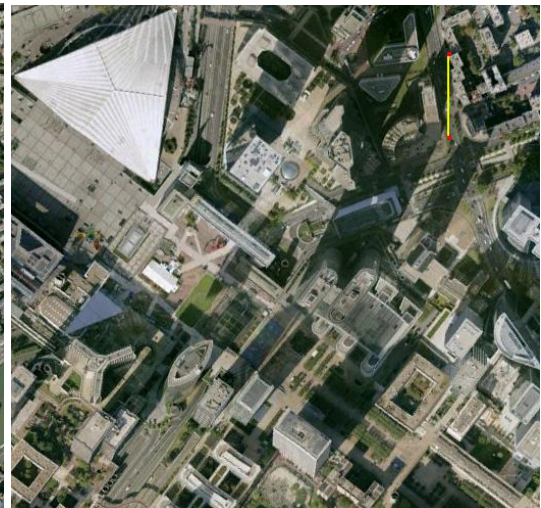
³ <http://www.infrared-thermography.com/material.htm>

⁴ Ref. Tab. 15, p.38, EPA report 2009

⁵ Table 5, EPA report, p. 15

⁶ Ref. Tab. 10, p.23, EPA report 2009

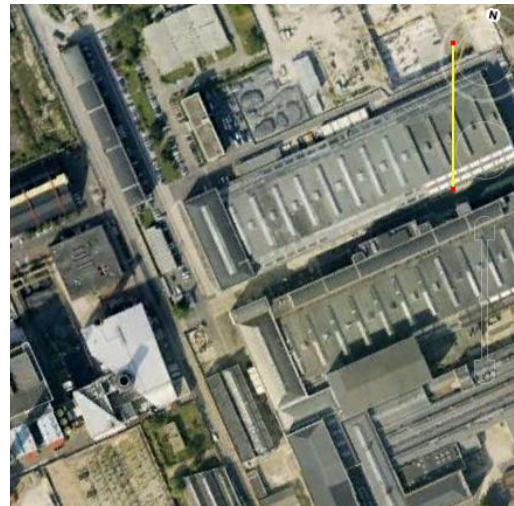
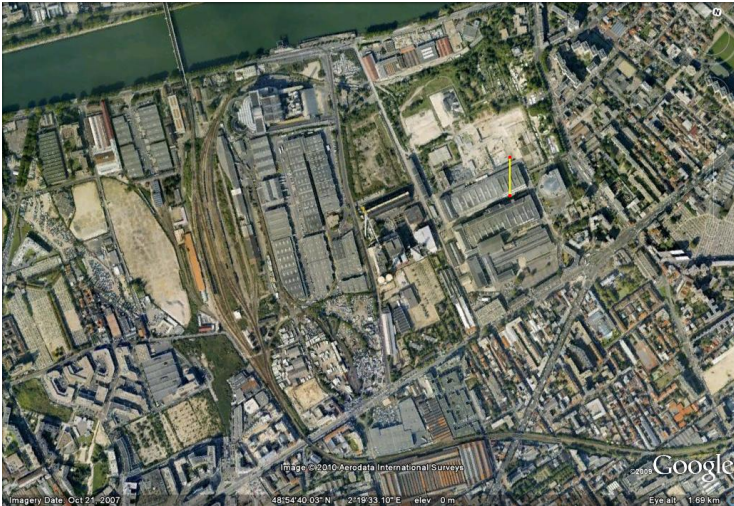
Depending on selected type of the surface different materials can be used at construction of buildings and streets. These materials were also taken into account. The thermal diffusivity was calculated based on weighting average of materials' diffusivities used for construction of buildings' walls and roofs. As construction materials the brick, wood, and glass were considered for the rural areas (RUR); the concrete, steel, and glass – for the ICD, CC, and HBD districts with different percentage contributions; and brick, wood/steel, and glass – for the RUR district. For simplicity, the thermal diffusivity of the ground surface was assumed same in all types of districts. Temperature inside the buildings is given behind the wall and roof surfaces. In general, a number of street directions (for each urban district) assumed to be equal 2. A street length was fixed to a greater value (100000 m) compared with modeling horizontal grid-cell. Orientation of the streets is assumed as NE-SW (45 deg or 0.785 radian) and SE-NW (135 deg or 2.355 radian). A number of height levels selected depended on the model resolution, assuming that the 1st model level is approximately 33 m (which also is a function of variability of meteorological variables), and the 2nd is 97 m (3rd and 4th are 176 and 268 m, respectively). Hence, a probability that buildings with such height might be presented within the height level of the model was also estimated.



City Center (CC)



High Buildings District (HBD)



Industrial Commercial District (ICD)



Residential District (RD)



Rural Area (RUR)

Figure 2.2.5.2: Examples of urban districts (extracted from Google-Earth) for the Paris metropolitan area and surroundings.

2.3. Meteorology Analysis and Selection of Specific Cases/Dates

In order to study in more details the chemical transport and link with dominating meteorological conditions during the selected episodes, the necessary materials were extracted from the international and DMI synoptic archives. These included the surface maps (covering most of the Europe), vertical sounding diagrams, and observations at selected World Meteorological Organization, WMO (#) synoptical stations covering periods: 1-31 July 2009 and 15 Jan – 14 Feb 2010. For selected synoptical stations – Paris-Orly (#07419; 48.7167°N, 2.3844°E, 89 m asl), Troyes-Barbery (#07168; 48.3167°N, 4.0167°E, 112 m), Chartres (#07143; 48.4603°N, 1.5011°E, 156 m), Bourges (#07255; 47.0581°N, 2.3703°E, 166 m), and Beauvais-Tille (#07055; 49.4468°N, 2.1285°E, 89 m) located in the center, to the east, west, south, and north directions of Paris, respectively (see Figure 2.3.1) – a set of corresponding meteorological observations was extracted and analyzed at 6 hour interval (e.g. 00, 06, 12, 18 UTCs) for both periods. These included the wind speed and direction, relative humidity, cloud cover, and precipitation in order to identify dominating atmospheric transport patterns and likelihood of removal processes from the atmosphere.

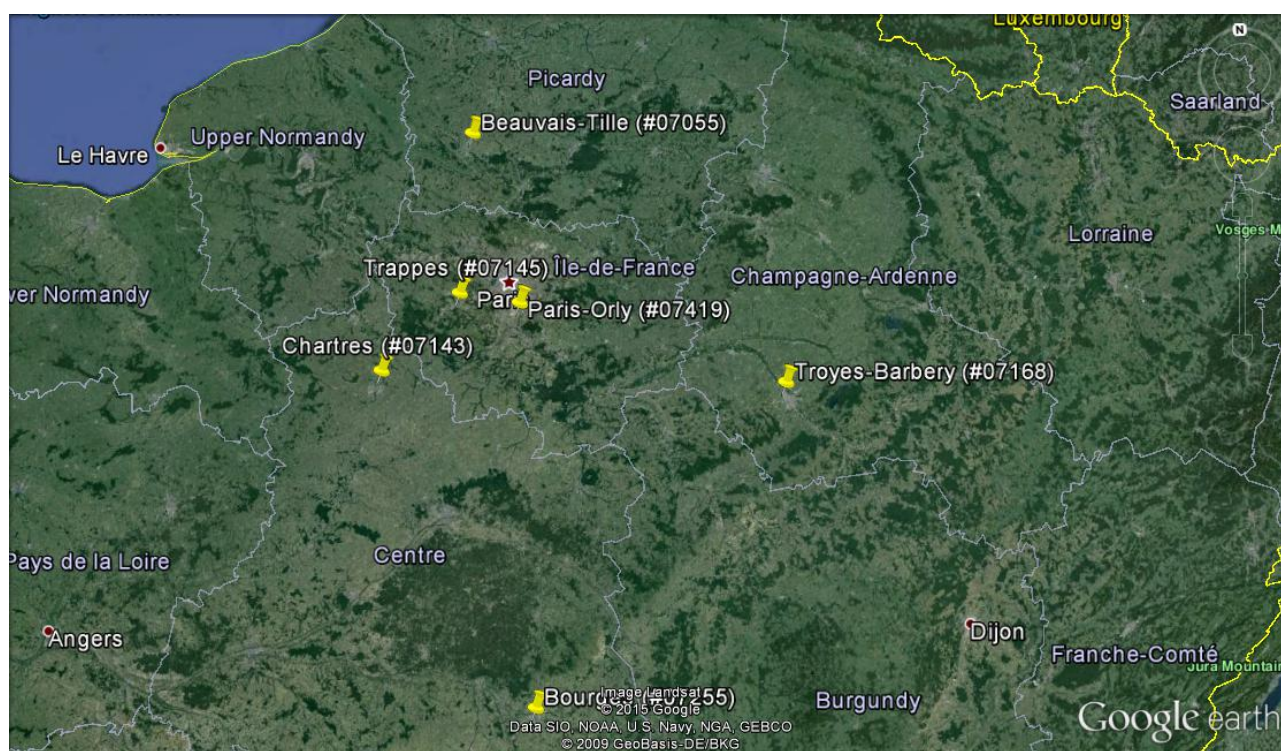


Figure 2.3.1: Geographical locations /extracted from Google-Earth/ of the WMO synoptical and vertical sounding measurement stations (all located in France).

In addition, the vertical sounding data/ profiles at the Trappes (#07145; 48.7706°N, 2.0083°E, 168 m; see Figure 2.3.1) station performed twice per day (at 00 and 12 UTCs) were also extracted. These were analyzed in order to identify/select dates/cases with dominating low wind conditions (LWC; among others such as typical – TWC and high wind – HWC), and observed vertical distribution of isothermal layers as layers having constant temperature with height. Such dates could be more representative for evaluation of the urban areas impact on both meteorology and chemistry. A summary for both measurement periods is shown in Appendix A1. As seen in the Appendix, the LWC was the dominating situation during the majority days of the MEGAPOLI measurement campaign. Moreover, as expected, more frequently the isothermal layers were observed in the troposphere during nighttime (e.g. at 00 UTC) compared with daytime soundings. Among all (62 as

2 UTC terms x 31 days) summer 2009 cases, there are only 7 were attributed to typical wind conditions (TWC), and hence, about almost 90% of all cases are linked with LWCs dates. Similarly, among all winter 2010 cases, there are only 4 were attributed to TWCs, and hence, more than 93% of all cases are linked with LWCs dates. The LWCs were the dominated type during both periods of the measurements, and hence, these are in major focus in this study.

Analyses of synoptical situation and time-series of observations at selected synoptical stations during both periods (summer and winter) showed domination of low-to-typical wind conditions over larger territories of inland France, and in particular, within the boundaries of the P01 domain. A summary is given in Table 2.3.1 (in Appendix 2 - example of atmospheric pressure and air temperature fields at 850 hPa level on as selected date of 3-4 Jul 2009).

As seen in the Table the western wind directions dominated during the summer period for about 60-68% of the time (on average with winds blowing from the south-west). On average, the relative humidity at stations varied within 64-70% reaching maximum of 97% and minimum of 8%. Mostly the cloud cover was less than 3, although at the Paris-Orly station it was more than 1.5 times higher (e.g. 4.8). At this station of the Paris megacity the cloud-free cases were observed less frequently (e.g. 16% of the time) compared with other stations where it was between 51-61% of the time. Moreover, between 76-90% of the time the precipitation was not observed at selected synop stations.

Table 2.3.1: Selected statistics on time-series of meteorological parameters (wind direction, relative humidity, cloud cover, and precipitation) at 5 French synoptical stations for the summer and winter measurement periods.

MetParameter	Wind Direction		Rel. Humidity	Cloud Cover		Precipitation	
	avg (in deg)	western dirs (in % of time)	avg/max/min (in %)	avg	no clouds (in % of time)	avg / max (in mm/6h)	not observed (in % of time)
<i>Synop Station</i>							
Summer measurement period: 1-31 Jul 2009							
<i>Paris-Orly</i>	225	67.7	64/93/25	4.8	16.1	0.15/ 6	82.3
<i>Troyes-Barbery</i>	226	59.7	68/97/32	2.5	55.7	0.17/ 9	83.1
<i>Chartres</i>	237	65.3	66/95/19	-	-	0.15/ 7	89.5
<i>Bourges</i>	225	64.5	65/97/21	2.4	61.3	0.68/ 69	81.5
<i>Beauvais-Tille</i>	226	66.1	70/96/8	2.9	50.8	0.37/ 13	75.8
Winter measurement period: 15 Jan – 14 Feb 2010							
<i>Paris-Orly</i>	167	41.9	85/100/20	6.5	8.1	0.89/ 91	66.9
<i>Troyes-Barbery</i>	187	34.7	85/98/7	3.5	53.2	0.93/ 89	70.9
<i>Chartres</i>	165	37.9	87/100/9	3.7	43.5	0.20/ 4	70.9
<i>Bourges</i>	159	38.7	87/100/67	3.3	55.7	0.24/ 8	77.4
<i>Beauvais-Tille</i>	182	41.1	90/100/8	5.6	33.9	0.22/ 3	62.9

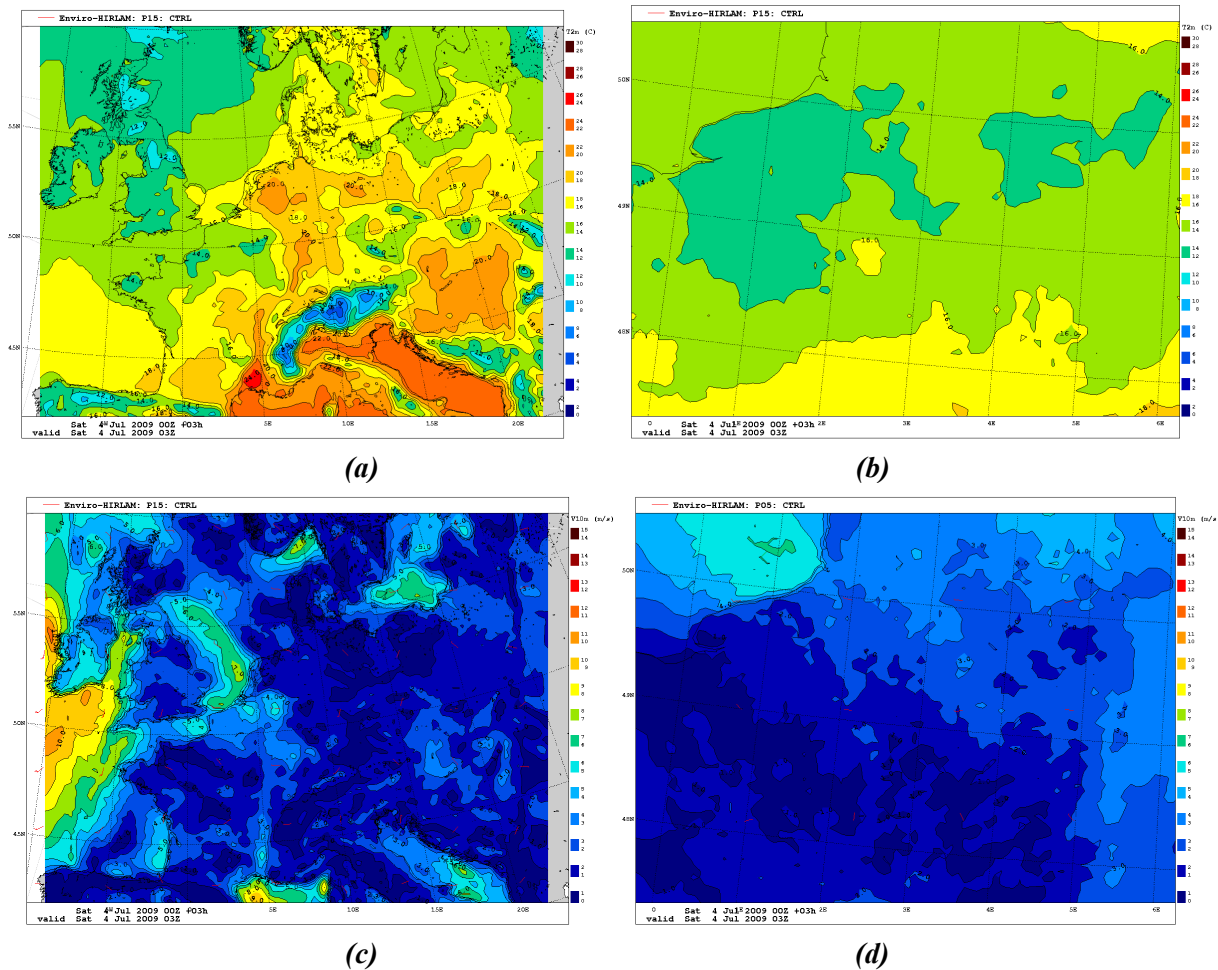
During the winter period, the dominating average wind direction was associated with the southern sector, the western wind directions became less frequent (e.g. reducing in frequency down to 34-42% of the time compared with the summer period). On average, the relative humidity at stations varied within 85-90% reaching maximum of 100% and minimum of 7%. The cloud cover was more than 3, and even higher at Paris-Orly (6.5) and Beauvais-Tille (5.6) stations located close to center

and north of the Paris metropolitan area. For these two stations the number cloud-free cases was also the lowest, as for other stations - it varied within 44-56% of the time. Finally, between 63-77% of the time the precipitation was not observed at these five synoptical stations.

2.4. Downscaling Meteorology

In order to run the Enviro-HIRLAM model over the first domain (P15) in a downscaling chain, the meteorological boundary conditions (BCs) from the European Center for Medium-range Weather Forecast (ECMWF) were extracted. These data are provided at horizontal resolution of 0.25 x 0.25 deg of latitude vs. longitude, at every 6 hour time interval, and at 60 vertical levels. Note, there are plans at ECMWF for the nearest future - to increase a horizontal resolution up to 0.15 deg and increase a number of vertical levels up to 90.

In our study, for the crudest (e.g. at 15 km resolution) Enviro-HIRLAM model run these meteorological data were pre-processed, e.g. interpolated vertically and horizontally according to the P15 domain specification (see Table in Figure 2.1.3.2). At finer scale runs (e.g. for 5 and 2.5 km resolutions) the meteorological BCs were taken from the outer model runs (e.g. from P15 run for P05 run, and from P05 run for P01 run, correspondingly). An example of such downscaling for P15-P05 is shown in Figure 2.4.1 for the selected meteorological parameters such as air temperature and relative humidity at 2m and wind speed at 10m.



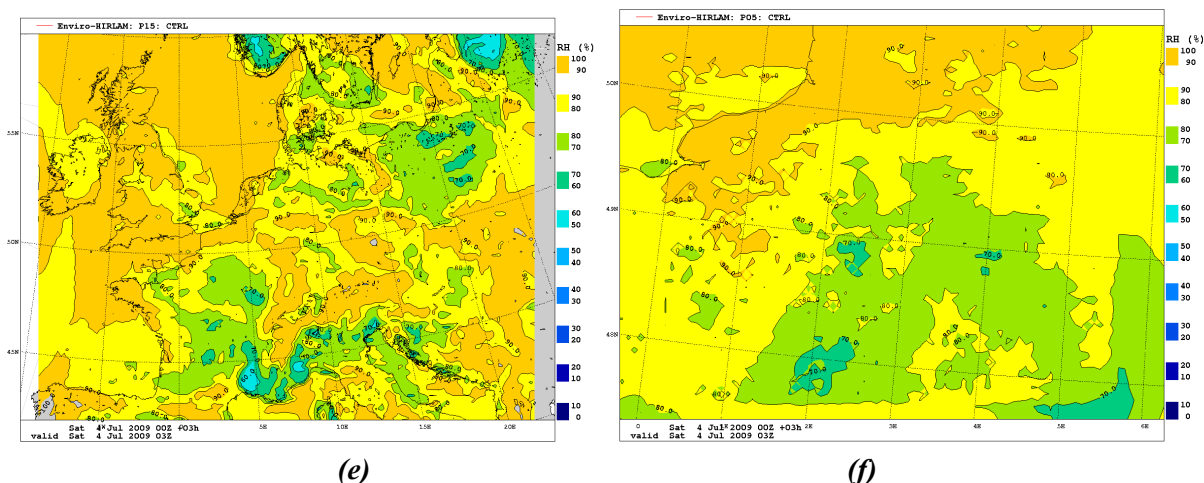


Figure 2.4.1: Example of the downscaling run for the Enviro-HIRLAM model domains (left column - from P15 to P05 – right column) for meteorology for (ab) air temperature at 2m, (cd) wind speed at 10 m, and (ef) relative humidity at 2m on 4 Jul 2009, 03 UTC.

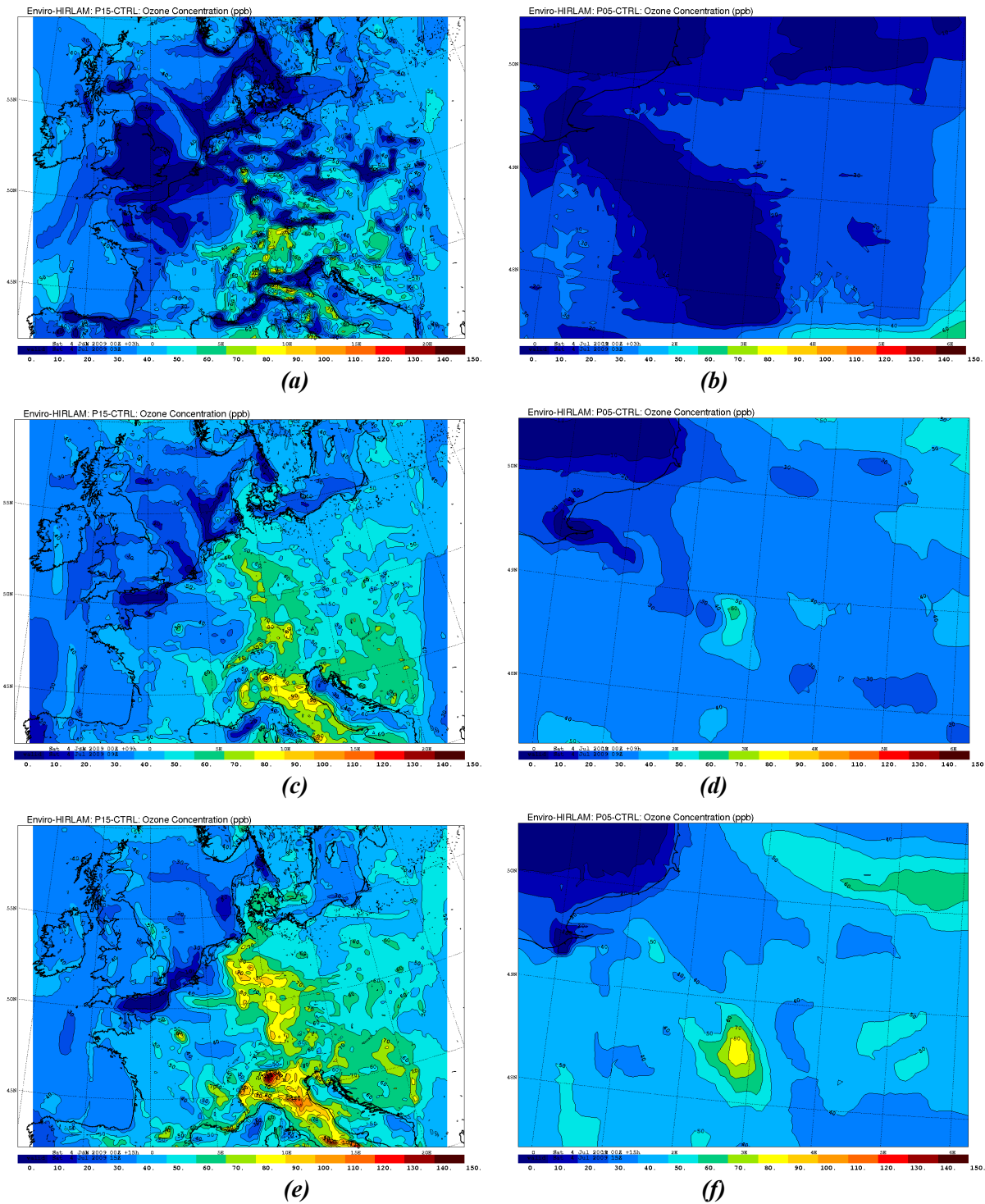
As seen, for the Enviro-HIRLAM-P15 runs the synoptical scale features, representing general patterns of spatio-temporal distribution of heat, momentum and moisture, are well re-produced at the European scale. At P05 runs (with 3 times higher resolution than P15) the role of meso-scale features became more visible compared with P15 runs, where the isolines of meteorological parameters are more smoothed. For P05 runs, more “irregularities” are appearing over the same geographical area in the P05 vs. P15 domains. The situation became even more complex when the downscaling is taking place for the finest P01 run (*see further sections in Results and Discussions*), because small-scale features and peculiarities (such as more sharper changes in orography, increased number of grid cells having larger fraction of urban class, re-distribution of different land-cover/land use categories, etc.) including those linked to influence of urban areas (due to morphology, anthropogenic heat, etc.) will start to play their own role.

2.5. Downscaling Chemistry

Similarly to downscaling of meteorology, the downscaling of chemical species fields was also performed for the same three domains. The list of chemical species being a part of the chemical mechanism in the model is shown in Appendix A3 (with a description, molecular/ chemical formulae and a remark on ID-number of the parameter used to save in output grib-file together with meteorological parameters). For the crudest (at 15 km resolution) Enviro-HIRLAM model runs the chemical boundary conditions (BCs) were pre-processed based on used MEGAPOLI emission datasets. For the finer (5 and 2.5 km) the chemical BCs were taken from the outer model runs (e.g. from P15 run for P05 run, and from P05 run for P01 run). Moreover, note that at initialization step, the pre-processing of the MEGAPOLI emissions (at resolution of 0.12 x 0.06 deg) - anthropogenic and natural (fire - Global Fire Emissions Database, GFEDv3 at resolution of 0.5 x 0.5 deg & biogenic, at resolution of 1 x 1 deg) – was performed for all model domains. The re-scaling coefficients to account correction on areal sources were taking into account as well in order to reflect changes in horizontal resolution of the nested runs vs. resolution of emission datasets.

An example of such downscaling for P15-P05 is shown in Figure 2.5.1 for one of selected chemical species – ozone (O₃) as pollutant. As seen, for the Enviro-HIRLAM-P15 run, the general patterns of ozone spatio-temporal distribution - with a dependence on potential sources of emissions, maritime vs. continental areas, and diurnal cycle behavior - are relatively well produced. The simulated meteorological fields are used as input at the same time step (because the Enviro-HIRLAM model

is online integrated) for processing/ modelling of atmospheric transport, dispersion, deposition, and chemical reactions of chemical species. As meteorology is changing on every time step, the chemistry will change correspondingly too. First of all, changes in wind patterns (from dominating synoptic scale to meso-scale and further to urban/local scale) on a diurnal cycle will change a spatial shape of “pollution cloud” and geographical location of possible maxima of ozone concentration as well as its magnitude (as both seen for P05 run in Figure 2.5.1dfh), but at the same time will keep a background averaged concentration at a relatively similar level.



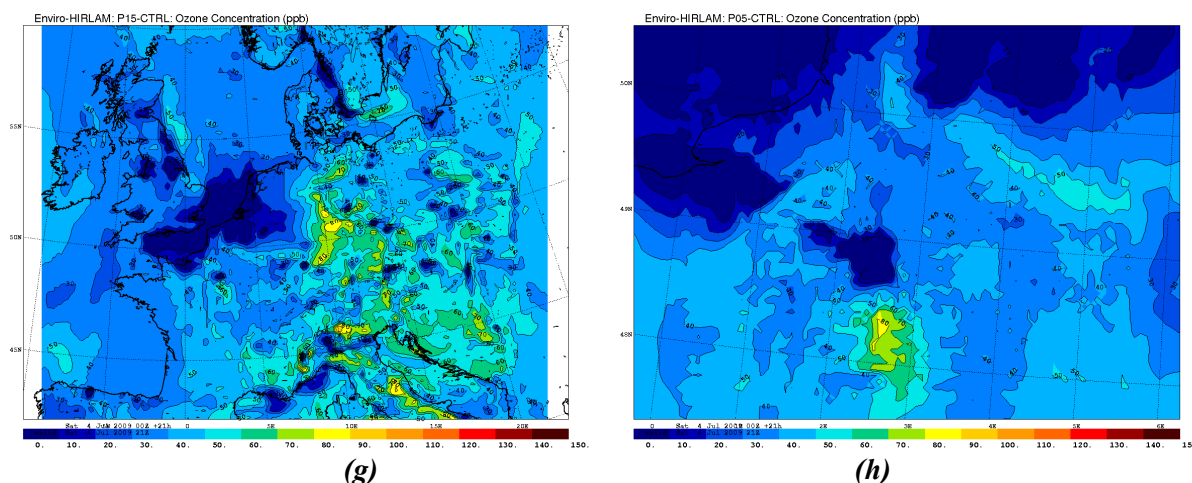


Figure 2.5.1: Example of the downscaling run for the Enviro-HIRLAM model domains (left column - from P15 to P05 – right column) for chemistry, e.g. ozone O_3 on a diurnal cycle at: (ab) 03, (cd) 09, (ef) 15, and (gh) 21 UTCs on 4 Jul 2009.

Observed changes in air temperature, pressure and relative humidity on a diurnal cycle could influence chemical reactions as well. Increased precipitation and humidity over selected grid cells could lead to a more efficient removal of pollution from the atmosphere on the underlying surface. The situation became more interesting and complex when the downscaling is taking place for the finest P01 run (see further sections in *Results and Discussions*), where changed meteorology at finer scales and urban areas will be playing their roles.

3. Results and Discussions

In this study, several typical specific cases/dates (during July 2009 and January-February 2010) were run employing the Enviro-HIRLAM model in a downscaling chain (P15-P05-P01). In runs in all grid cells, where the urban class was presented in the modeling domain, the BEP module was activated for calculations. In addition, typical values of AHFs from the Large scale Urban Consumption of energy (LUCY; Allen *et al.*, 2010) model were extracted for the Paris metropolitan area and included as a part of the urban module. In all other non-urban grid cells the ISBA scheme calculations were applied. In this section, analysis on examples is shown. The meteorological and chemical fields' simulations for the urbanized areas were driven using boundary conditions generated by the Enviro-HIRLAM-P05 model (at 5 km horizontal resolution). These conditions were used as input for simulation with the Enviro-HIRLAM-P01 model (control and urbanized versions) and of higher resolution.

For specific dates within the two studied periods, two independent types of the model runs were performed: 1) control run (reference - i.e. no modifications in the ISBA scheme); and 2) modified runs with urban module activated (having different options included). Variability of meteorological parameters such as air temperature and relative humidity (at 2 m), surface temperature, wind velocity (at 10 m), cloud cover, boundary layer height, as well as concentrations of selected chemical species (with focus on ozone) were analyzed comparing outputs of the control run vs. runs with modified parameters.

3.1. Air Temperature at 2m

The variability of the air temperature at 2m on a diurnal cycle is shown in Figure 3.1.1 for the control (Fig. 3.1.1ac) vs. modified (Fig. 3.1.1bd) runs of the model. As seen, at noon (12 UTC)

there are some but not large differences between the runs, as the area is enclosed by the same temperature isoline, although it has more well-shaped form for urbanized run compared with the control, where it has a more irregular pattern and does not well represent the Paris urban area. In general, when the urban effects are included, these differences are more observed during late evening - night - early morning time hours, with the largest – during nighttime as shown as example in Figure 3.1.2d. This shows effect of the so-called Urban Heat Island (UHI) which clearly underlines that the Paris metropolitan area is significantly warmer than the surrounding rural areas, and such effect is also best pronounced during summer and winter days, and especially under the low wind conditions.

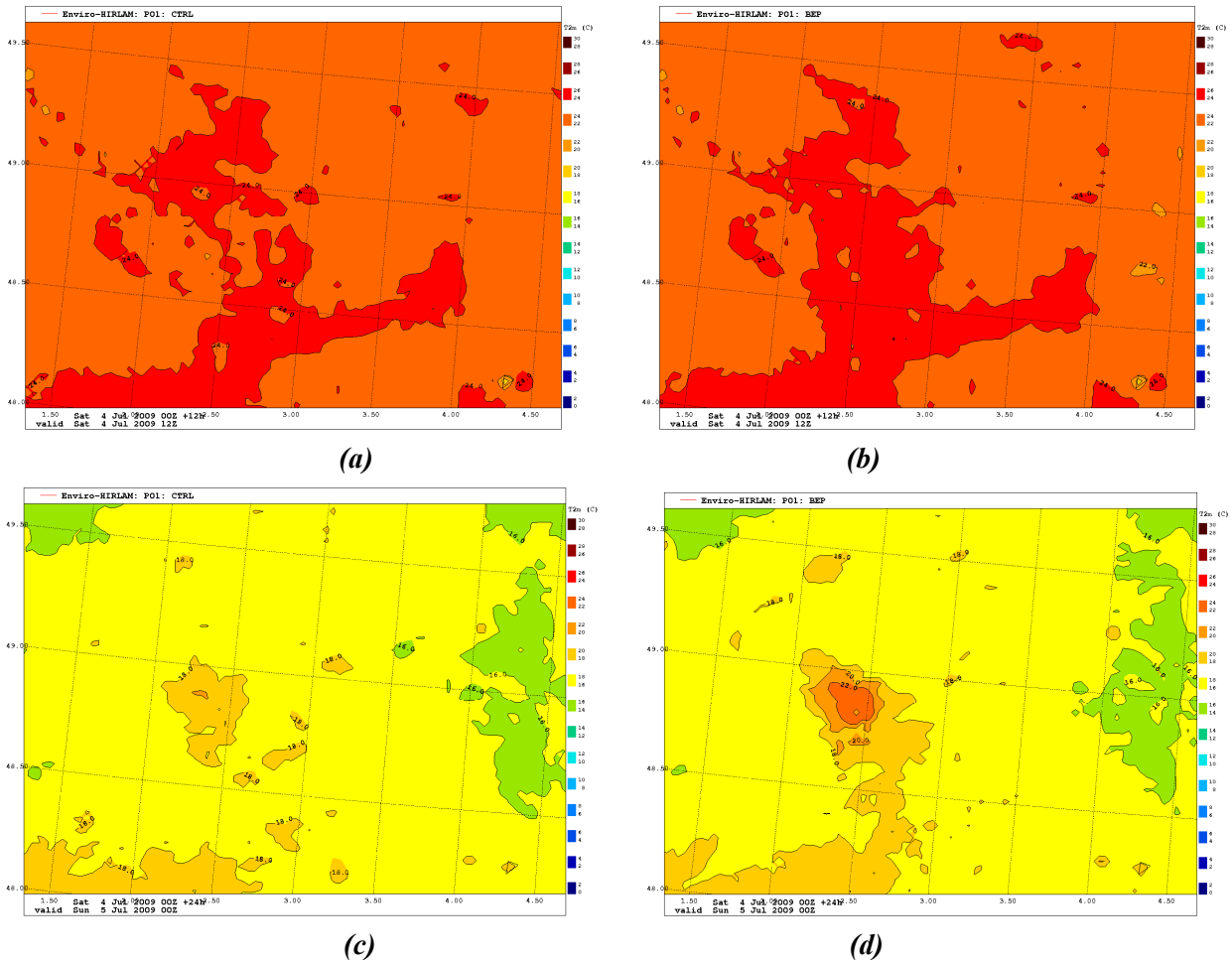


Figure 3.1.1: Variability of the air temperature at 2m on a diurnal cycle – for the control (left column – a-c) vs. urbanized (right column – b-d) Enviro-HIRLAM-P01 model runs - at (ab) 12 UTC on 4 Jul 2009 and (cd) 00 UTC on 5 Jul 2009.

Moreover, as shown on example of the low wind conditions date, depending on additional changes in AHF (see Figure 3.1.2) the impact of the city or a so-called “foot-print” can be extended farther (in southern direction) as well as expanded in other directions increasing heat signature of the city and bringing a potential influence of the metropolitan area for more than a 100 km away from the city. The temperature differences between urban vs. rural areas became more evident reaching up to several degrees and clearly underling the Paris urban area with adjacent sub-urbans. The air temperature differences can reach up to 4°C (comparing enclosed isolines at AHFs of 100 vs. 250 W/m²). At higher AHFs, the total area enclosed by the highest temperature isoline became almost 4 times larger.

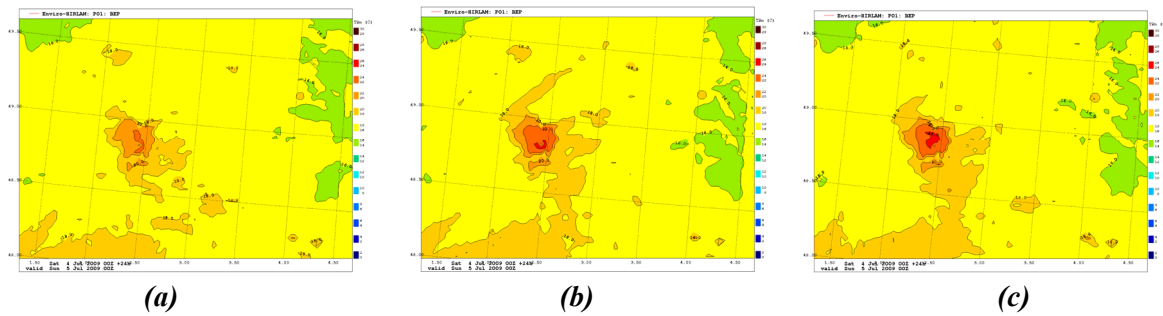


Figure 3.1.2: Enviro-HIRLAM-P01-urban run: Air temperature at 2m field on 5 Jul 2009, 00 UTC due to including additional variability in anthropogenic heat fluxes: (a) 100, (b) 200, and (c) 250 W/m^2 .

The difference (Enviro-HIRLAM-P01: control vs. urbanized runs) fields for the air temperature at 2m on a diurnal cycle are shown in Figure 3.1.3. The zoom over domain enlarged the Paris metropolitan area, and as seen, it is well identified as an area with the largest changes between the runs. The influence (up to 1-1.5°C) of the city on remote areas can be also identified (see Fig. 3.1.3, 06 UTC) and this had occurred due to light winds blowing into the south-eastern sector during the morning hours. These changes became larger (up to 3.5°C) during late evening – early morning hours, and almost negligible during daytime.

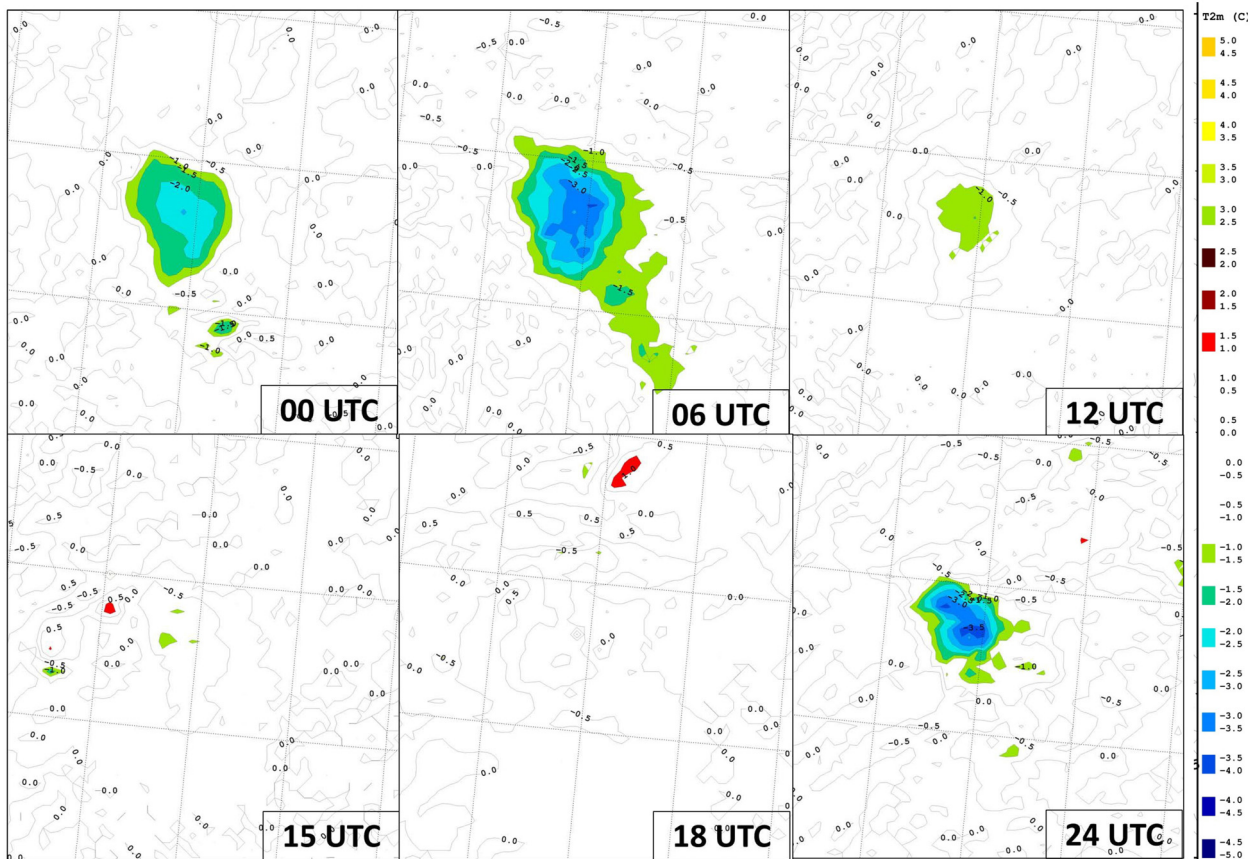


Figure 3.1.3: Paris metropolitan area: diurnal cycle variability of the difference fields (Enviro-HIRLAM-P01: control vs. urban runs) for air temperature at 2m on 4 Jul 2009 (from 00 till 24 UTCs).

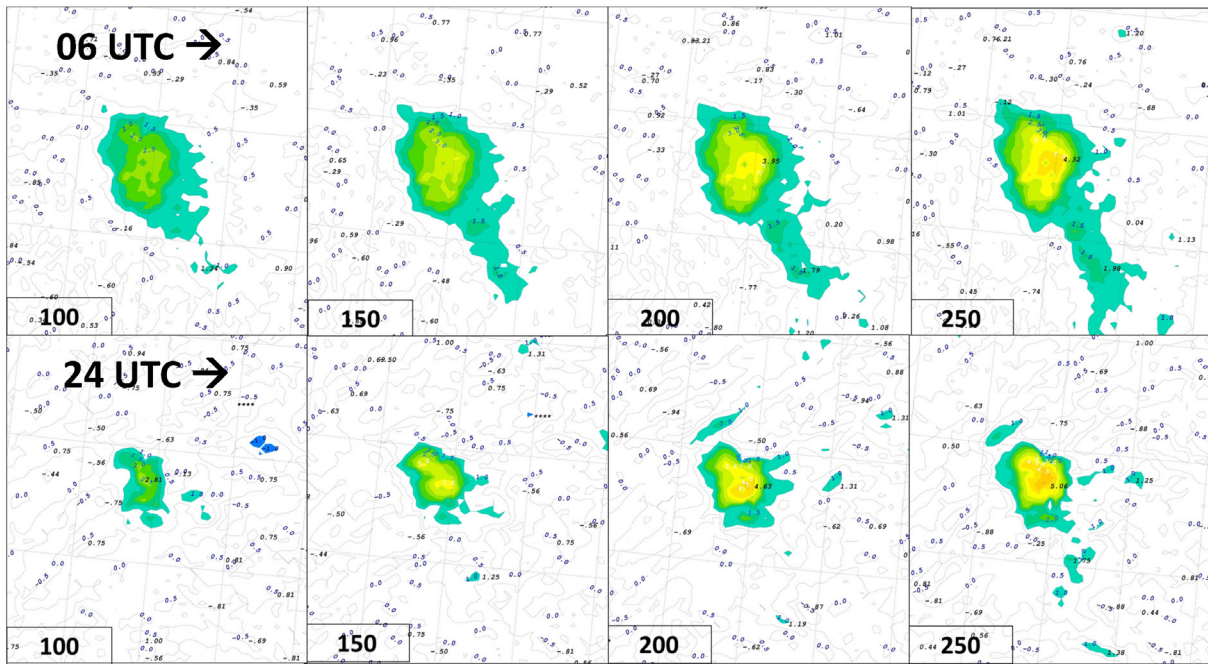
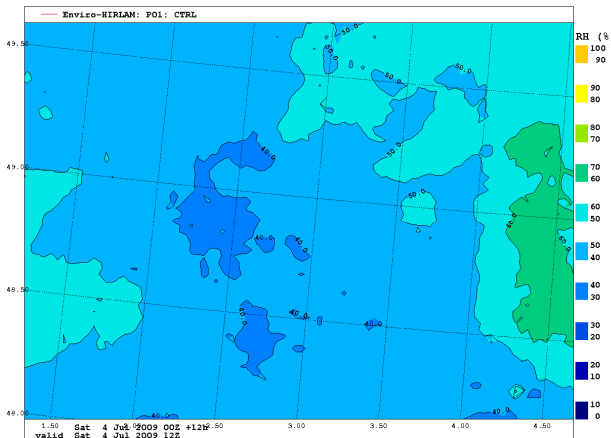


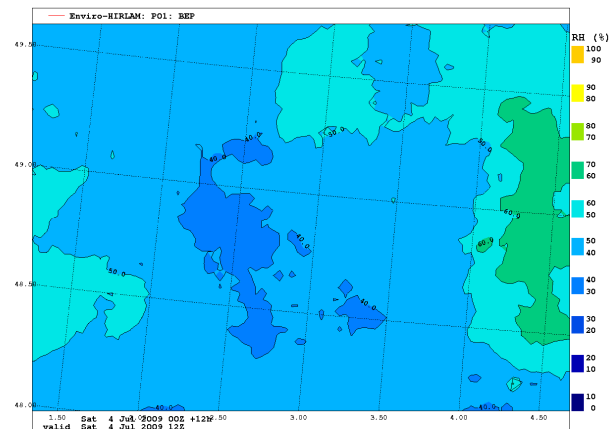
Figure 3.1.4: Paris metropolitan area: diurnal cycle variability of the difference fields (Enviro-HIRLAM-P01: urban vs. control runs) for air temperature at 2m with changing anthropogenic heat fluxes (100, 150, 200, and 250 W/m^2) on 4 Jul 2009 at 06 and 24 UTCs.

3.2. Relative Humidity at 2m

The variability of the relative humidity at 2m on a diurnal cycle is shown in Figure 3.2.1 for the control (Fig. 3.2.1ac) vs. modified (Fig. 3.2.1bd) runs of the Enviro-HIRLAM-P01 model. As seen, at noon (12 UTC) there are relatively minor differences between the runs, although area enclosed by the same isoline is slightly larger for the urbanized run. As seen, in both cases the value of the relative humidity is smaller comparing with surroundings (meaning that it is drier over the urban area compared with the rural areas). In a case of the P01-urban run, the area with lowered (by extra more than 10%) relative humidity values will be expanded, and the city became even more drier compared with the control run (Fig. 3.2.1cd).



(a)



(b)

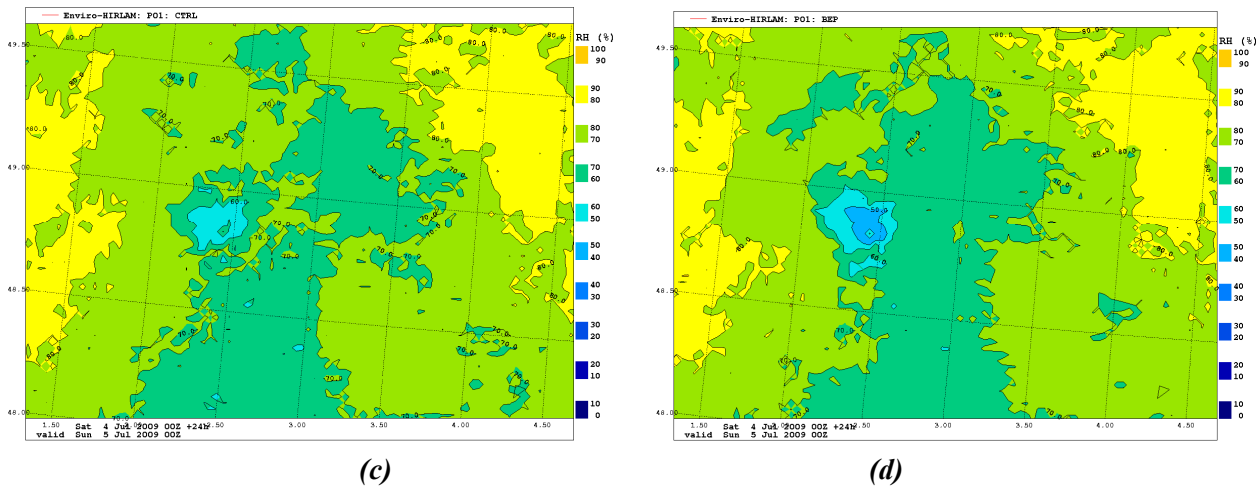


Figure 3.2.1: Variability of the relative humidity at 2m on a diurnal cycle – for the control (left column – a-c) vs. urbanized (right column – b-d) Enviro-HIRLAM-P01 model runs - at (ab) 12 UTC on 4 Jul 2009 and (cd) 00 UTC on 5 Jul 2009.

Additional changes in anthropogenic heat fluxes (see Fig. 3.2.2) could also lead to changes of boundaries where the Paris megacity impact on relative humidity field will be pronounced. As seen, with increasing AHFs values, there is also increase in spatial expansion of the impacted area as well as decrease in relative humidity value. All these also show the UHI effect, which clearly underlines that the Paris metropolitan area can be substantially drier than the surrounding rural areas, and such effect is better pronounced under the low wind conditions.

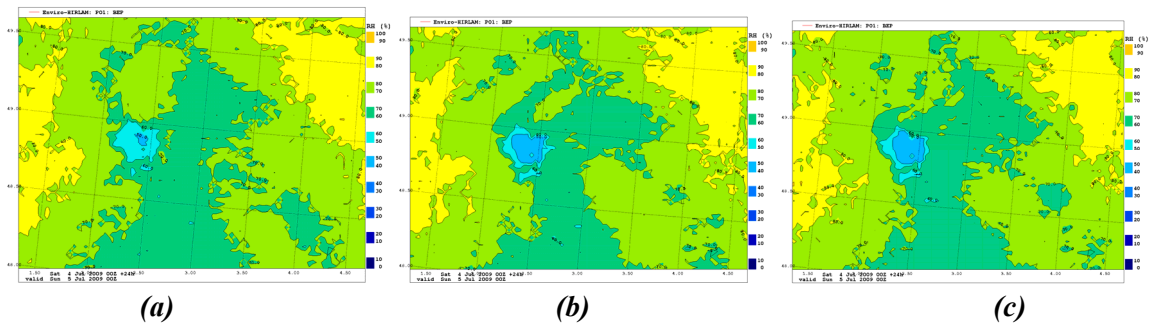


Figure 3.2.2: Enviro-HIRLAM-P01-urban run: Relative humidity at 2m on 5 Jul 2009, 00 UTC due to including additional variability in anthropogenic heat fluxes: (a) 100, (b) 200, (c) 250 W/m^2 .

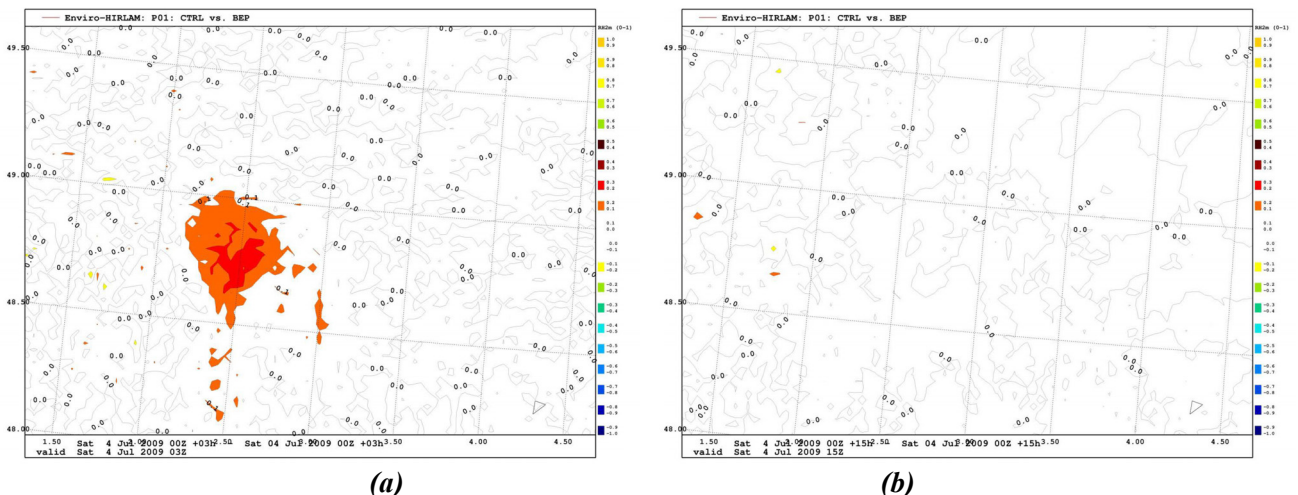
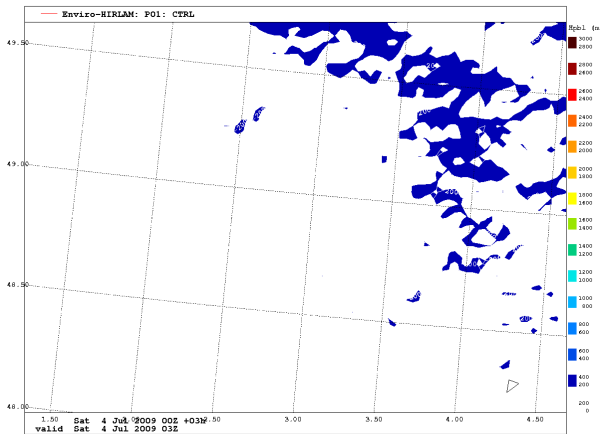


Figure 3.2.3: Paris metropolitan area: variability of the difference fields (Enviro-HIRLAM-P01: control vs. urban runs) for relative humidity at 2m at (a) 03 UTC and (b) 15 UTC on 4 Jul 2009.

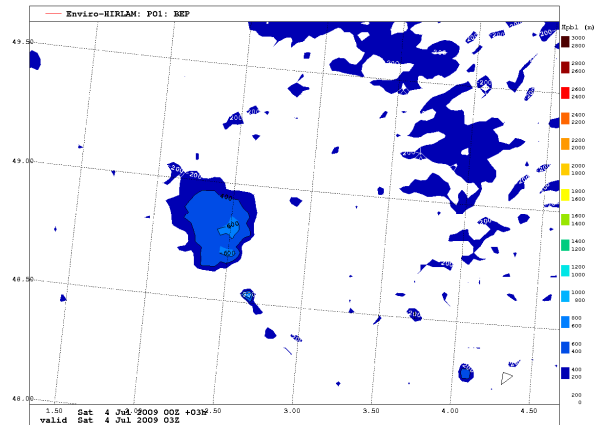
On a diurnal cycle, during late evening – nighttime hours the differences in relative humidity at 2m between the Enviro-HIRLAM-P01 (control vs. urbanized) runs can be up to 20% (0.2 on a scale shown below in Figure 3.2.3a), and for the rest of the day these changes were almost negligible.

3.3. Boundary Layer Height

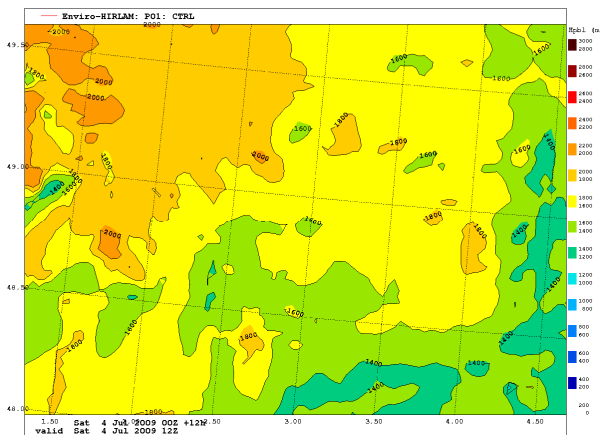
The variability of the boundary layer height on a diurnal cycle is shown in Figure 3.3.1 for the control (Fig. 3.3.1ace) vs. modified (Fig. 3.3.1bdf) runs of the model. As seen, for the control run the boundary layer height is not well reproduced, e.g. when the effects of the urban area are not taken into account. With urbanization included (see Fig. 3.3.1bdf), the “urban island” became more clearly visible (starting at late evening through nighttime hours) – the boundary layer height is increased over the megacity area as well as adjacent surroundings (sub-urban areas and smaller size cities). During daytime it is less pronounced although the differences are still visible (see Fig. 3.3.1d).



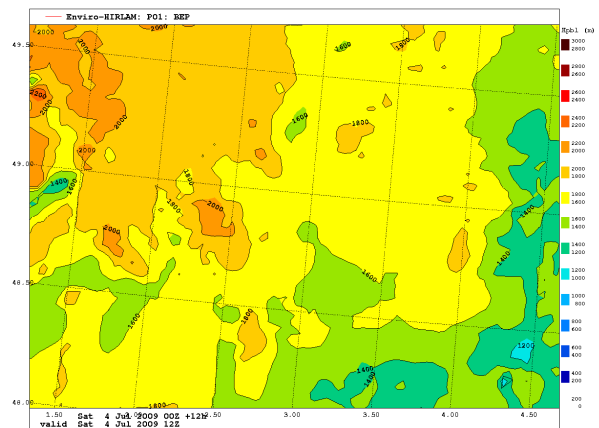
(a)



(b)



(c)



(d)

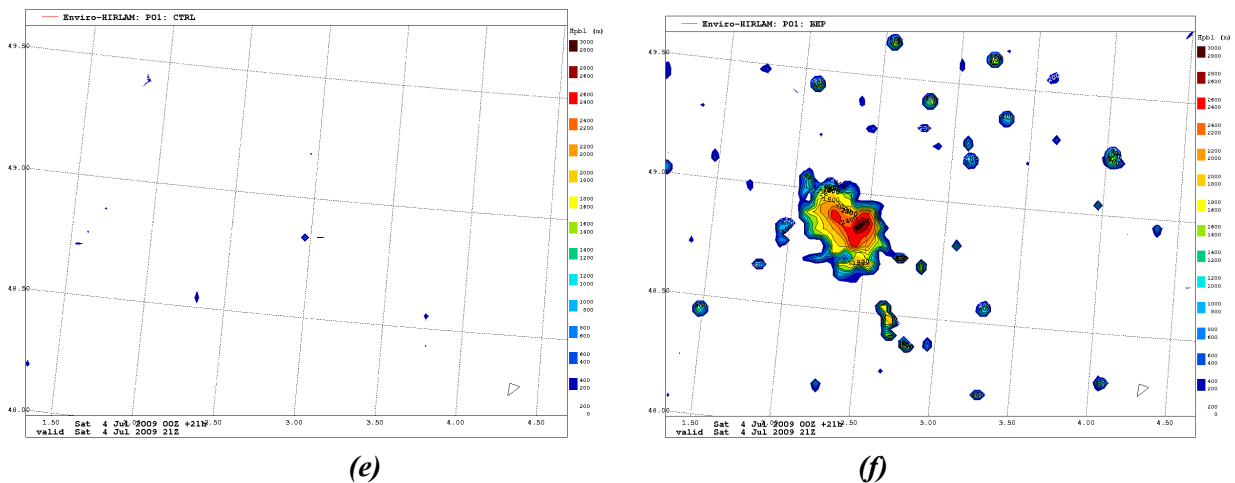


Figure 3.3.1: Variability of the boundary layer height on a diurnal cycle – for the control (left column – a-c-e) vs. urbanized (right column – b-d-f) Enviro-HIRLAM-P01 model runs - at (ab) 03, (cd) 12, and (ef) 21 UTCs on 4 Jul 2009.

Simulations also showed that for runs with different AHF values (ranging 100-200-250 W/m²) assigned to urban grid cells, both the “urban island” intensity and expansion of the boundaries are stronger and larger, respectively. With more intense anthropogenic heat fluxes, more urban areas (even relatively small urban settlements) will become affected (see Fig. 3.3.2c) with boundary layer height reaching more than 2.5 km at evening time.

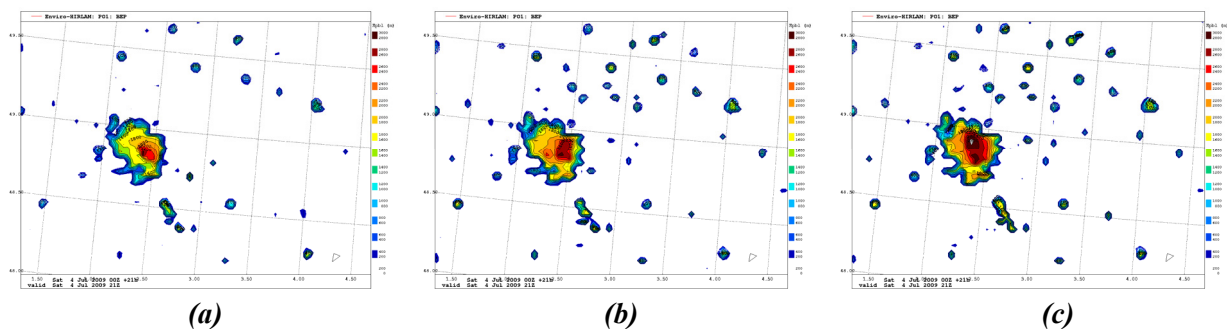


Figure 3.3.2: Enviro-HIRLAM-P01-urban run: Boundary layer height on 4 Jul 2009, 21 UTC due to including additional variability in anthropogenic heat fluxes: (a) 100, (b) 200, (c) 250 W/m².

3.4. Wind Speed at 10m

The variability of the wind speed at 10 m on a diurnal cycle is shown in Figure 3.4.1 for the control (Fig. 3.4.1ac) vs. modified (Fig. 3.4.1bd) runs of the model. As seen, for the control run there are no visible changes in wind speed over the metropolitan area, or when the effects of the urban area are not taken into account. With urbanization included (see Fig. 3.4.1bd), the influence of urban area became more clearly visible (and especially, at nighttime hours; see Fig. 3.4.1d) – the wind speed has changed over the megacity area and surroundings. During daytime it is less pronounced although the differences are still visible (see Fig. 3.4.1b).

On a diurnal cycle, as seen in Figure 3.4.2, the differences in wind speed are larger during late evening – nighttime – early morning hours, reaching up to 2.5-3 m/s over the most urbanized areas. During daytime, the differences are smaller – up to 1.5-2 m/s (with the lowest values at 09-12 UTCs). A total area where such differences are observed is varying significantly throughout the day as well when the impact of less urbanized and smaller by size cities is also observed.

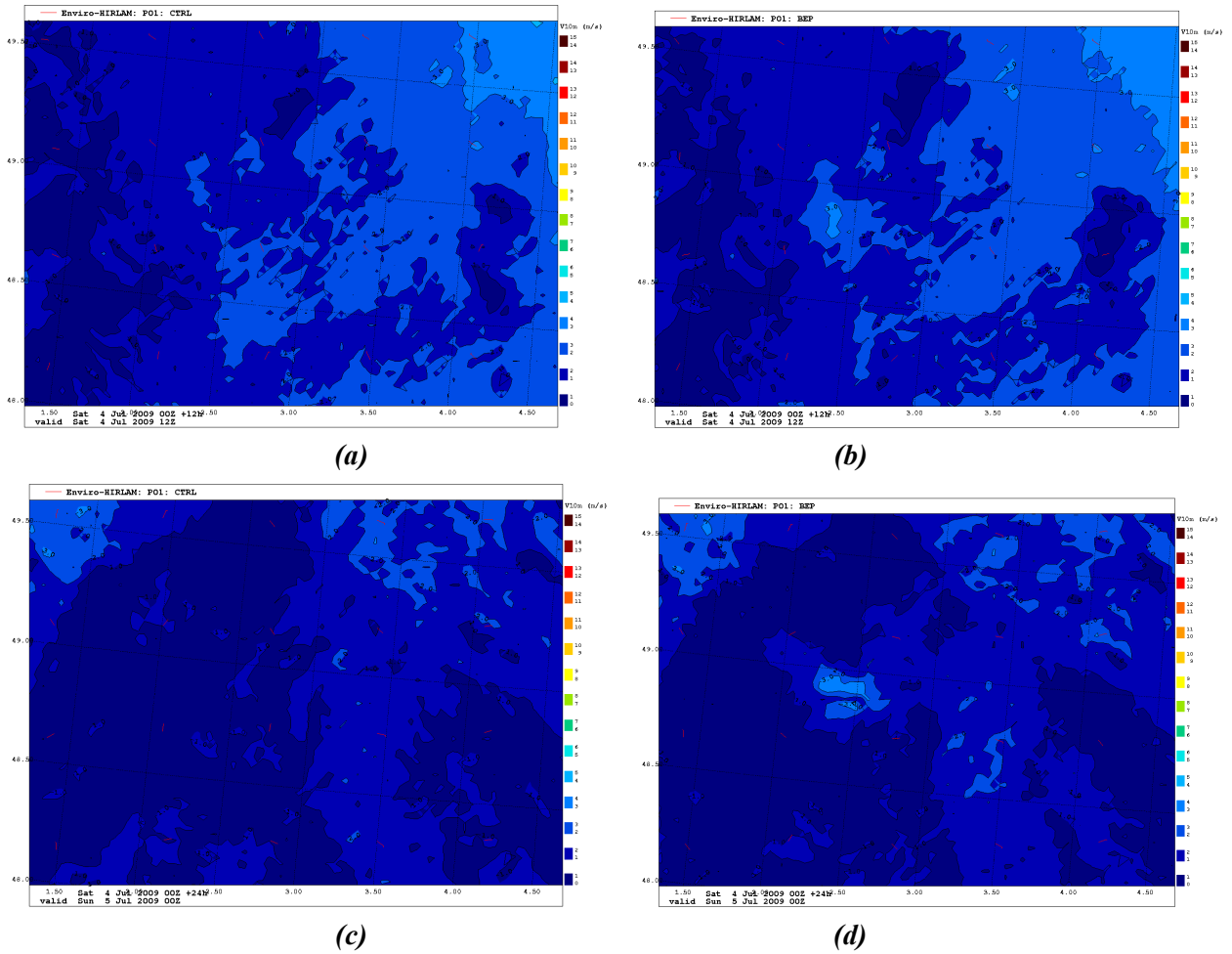


Figure 3.4.1: Variability of the wind speed at 10m on a diurnal cycle – for the control (left column – a-c) vs. urbanized (right column – b-d) Enviro-HIRLAM-P01 model runs - at (ab) 12 UTC on 4 Jul 2009 and (cd) 00 UTC on 5 Jul 2009.

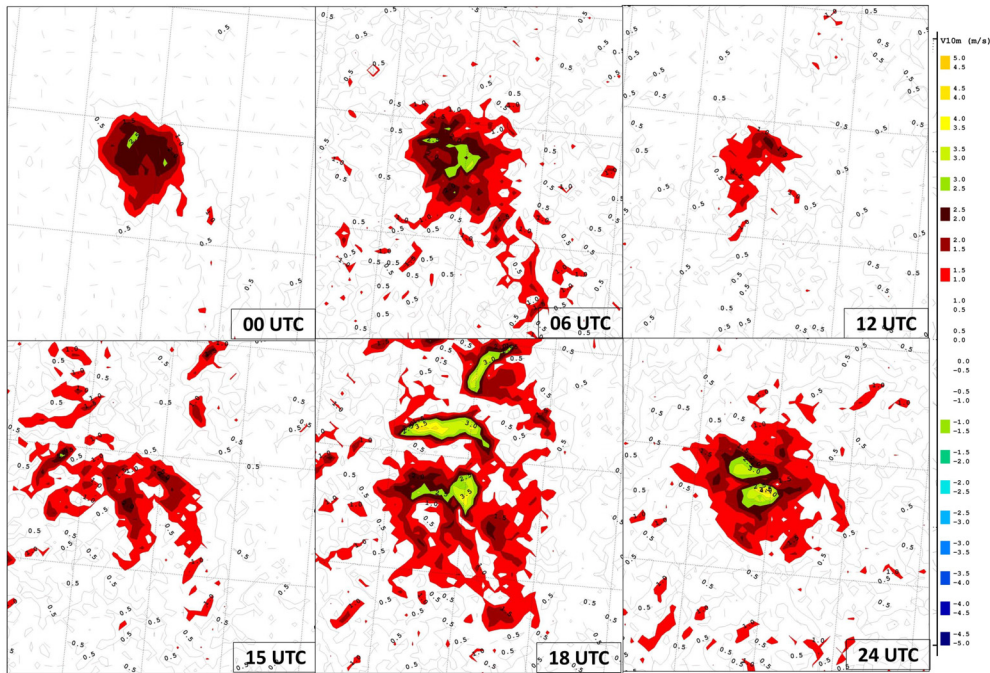


Figure 3.4.2: Paris metropolitan area: diurnal cycle variability of the difference fields (Enviro-HIRLAM-P01: control vs. urban runs) for wind speed at 10m on 4 Jul 2009 (from 00 till 24 UTCs).

3.5. Surface Temperature

The variability of the surface temperature on a diurnal cycle is shown in Figure 3.5.1 for the control (Fig. 3.5.1ac) vs. modified (Fig. 3.5.1bd) runs of the model. As seen, for the daytime at 12 UTC (Figs. 3.5.1ab) the territories with higher surface temperatures than the surroundings are observed in both cases, but the total area covered with higher temperatures is several times larger for the urbanized run compared with the control. It is also seen during the nighttime at 00 UTC as well (Figs. 3.5.1c vs. 3.5.1d). When urbanization is included, the influence of metropolitan area on the magnitude of surface temperature and its extension from the city boundaries into suburban and rural areas is more underlined and visible. The similar pattern for magnitude and extension is observed with increasing of AHF values as seen in Fig. 3.5.2abc – the higher is the AHF, than the larger is the surface temperature value and the larger will the total area, where such effect is observed.

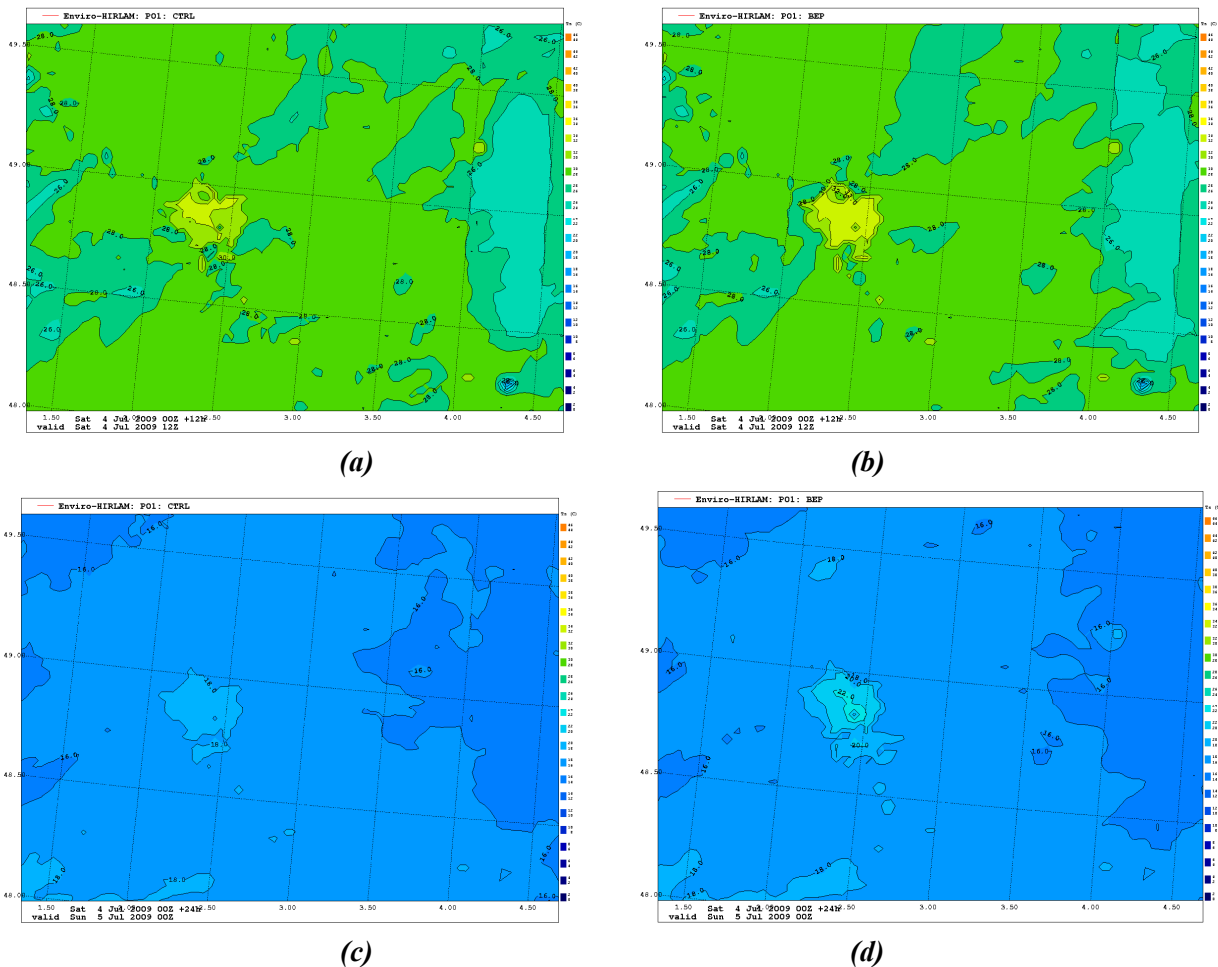


Figure 3.5.1: Variability of the surface temperature on a diurnal cycle – for the control (left column – a-c) vs. urbanized (right column – b-d) Enviro-HIRLAM-P01 model runs - at (ab) 12 UTC on 4 Jul 2009 and (cd) 00 UTC on 5 Jul 2009.

As seen in Figure 3.5.3, the differences between the runs are more pronounced (up to 2-3°C) and more localized over the Paris metropolitan area during nighttime – early morning hours. It shows that the modelled surface temperatures for the urbanized runs are higher compared with the control runs. And these difference, although are still visible, but of significantly smaller magnitude (up to 1°C) as well as small isolated cells which are distributed over the model domain reflecting changes of both signs (from -1 to +1.5°C) in suburban areas and smaller size cities.

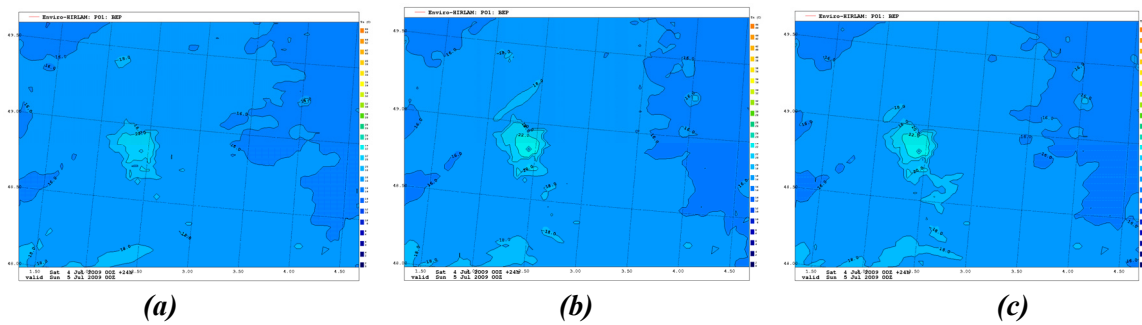


Figure 3.5.2: Enviro-HIRLAM-P01-urban run: Surface temperature on 5 Jul 2009, 00 UTC due to including additional variability in anthropogenic heat fluxes: (a) 100, (b) 200, (c) 250 W/m^2 .

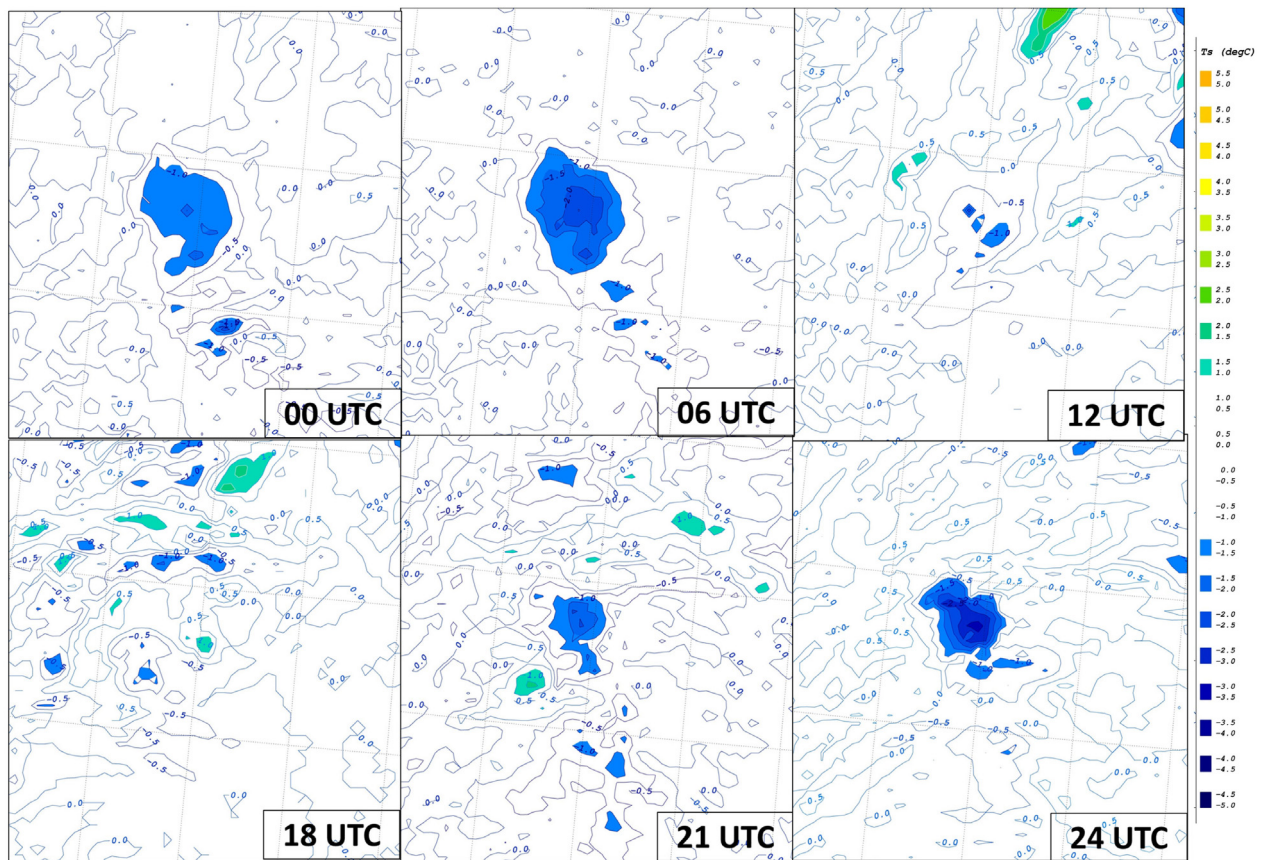


Figure 3.5.3: Paris metropolitan area: diurnal cycle variability of the difference fields (Enviro-HIRLAM-P01: control vs. urban runs) for the surface temperature on 4 Jul 2009 (from 00 till 24 UTCs).

3.6. Total Cloud Cover

The variability of the total cloud cover on a diurnal cycle is shown in Figure 3.6.1 for the control (Fig. 3.6.1a) vs. modified (Fig. 3.6.1b) runs of the model on example of 18 UTCs term. The propagation of cloud cover from the maritime and seashore territories of Atlantic is directed towards the east. The modelled cloud cover field has a spatially irregular pattern with isolated cloud patches over the western part of the model domain. Although patterns looks similar, but over the Paris metropolitan area there is significant difference: for the urbanized run (Fig. 3.6.1b) there is largely expanded area with increased values of the cloud cover (up to 100%), and that is not observed at all for the control run (see Fig. 3.6.1a). Moreover, it should be stressed that similar

pattern is observed with increasing of AHF as seen in Figs. 3.6.2abc. Such “spot” over the Paris and surroundings is observed and the area of such change is expanding with higher AHFs.

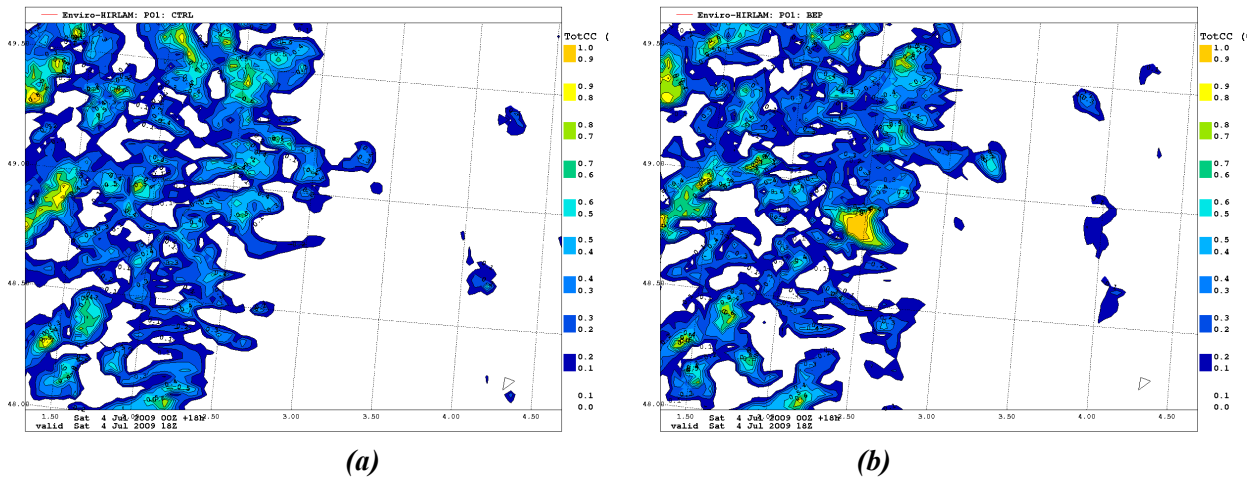


Figure 3.6.1: Variability of the total cloud cover for the control (a) vs. urbanized (b) Enviro-HIRLAM-P01 model run on 4 Jul 2009, 18 UTC.

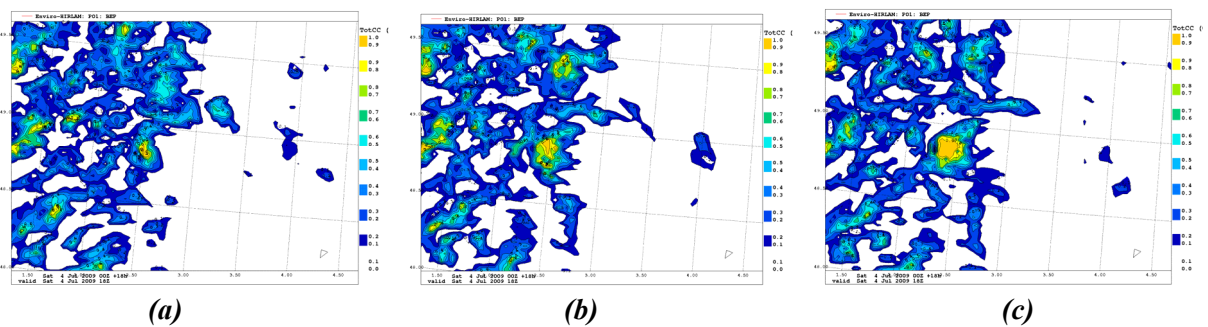
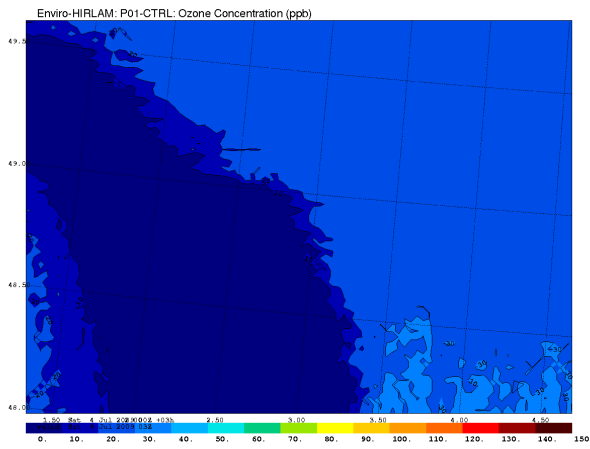


Figure 3.6.2: Enviro-HIRLAM-P01-urban run: Cloud cover on 4 Jul 2009, 18 UTC due to including additional variability in anthropogenic heat fluxes: (a) 100, (b) 200, (c) 250 W/m².

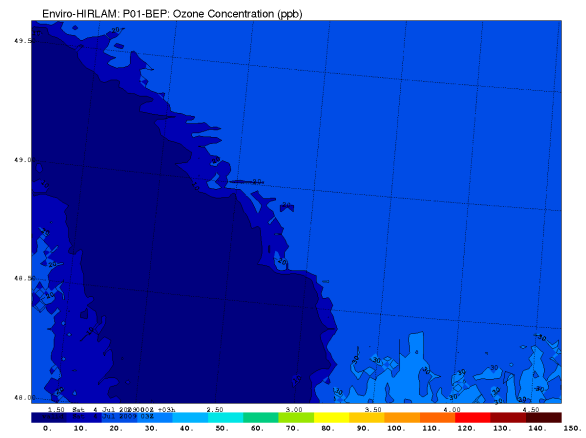
3.7. Ozone Concentration

The variability of the ozone concentration on a diurnal cycle is shown in Figure 3.7.1 at the lowest model level for the control (Fig. 3.7.1aceg) vs. modified (Fig. 3.7.1bdfh) runs of the model. As seen (Figs. 3.7.1ab), for the Paris metropolitan area and surroundings the ozone levels are similar for both runs at nighttime (03 UTC), but the area of the ozone pollution cloud is slightly less expanded in west-east direction for the urbanized run. The background concentration within high resolution domain is about 20 ppb, and within the metropolitan area it is lower than 10 ppb. At morning time (at 09 UTC, Figs. 3.7.1cd), a difference is seen in the southern part of the city, where the ozone cloud (having originally lower concentrations) is decreasing in size (due to increasing solar radiation and hence, speeding-up photochemical reactions) and also moving (due to lower wind dominating wind direction and increasing wind speed) towards the south border of the model domain, and in particular, along the river banks of industrial commercial districts of Paris (which are represented in the urban run). The ozone background concentration is increasing within the domain up to 30 ppb. At mid-day (at 15 UTC, Figs. 3.7.1ef), there are no significant differences in concentration between the runs, although for the urban run the isolines of ozone concentration field are more elongated in the south-eastern direction and less extended in west-east directions, showing a more narrowed concentration field along the Paris metropolitan areas and suburbs. At the same time the ozone background concentration continues to increase up to 40 ppb. At late evening hours (at 21 UTC, Figs. 3.7.1gh), the concentration started quickly to decrease (e.g. after sunset) although

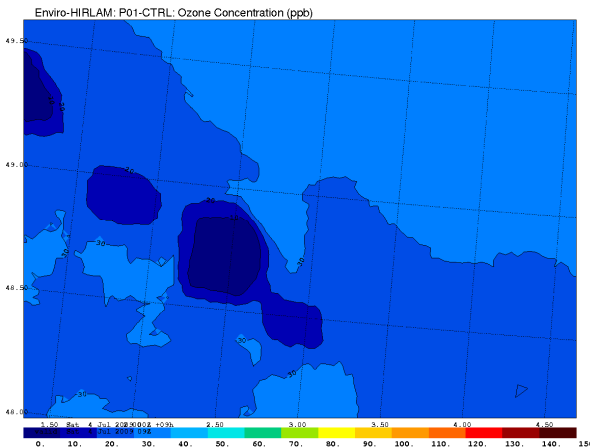
spatially such decrease is slower for the urban run. The background ozone concentration decreases also down to 30 ppb, and over the Paris and suburban areas down to 10 ppb.



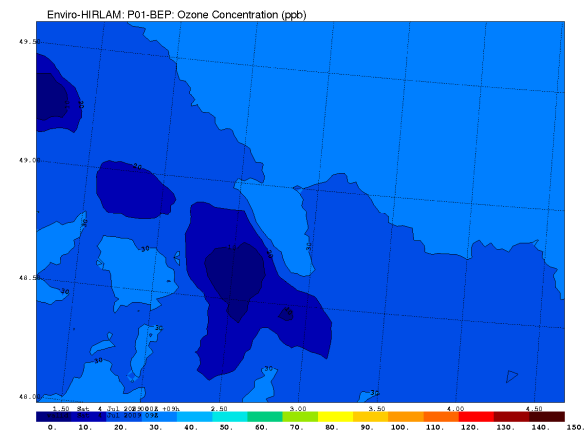
(a)



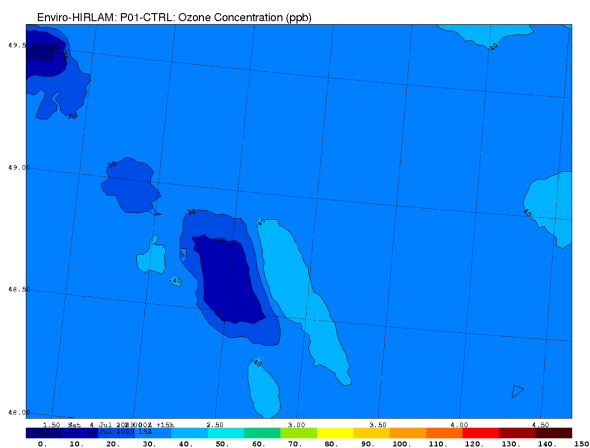
(b)



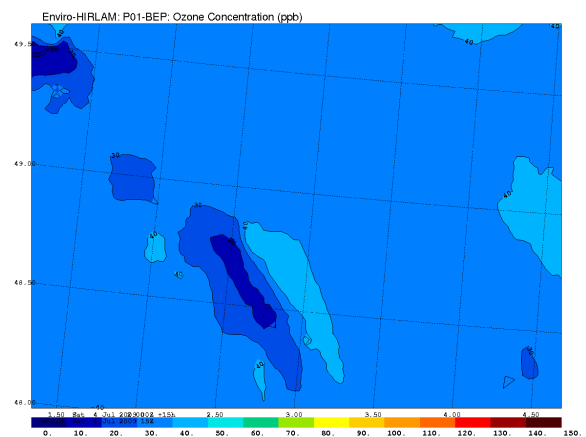
(c)



(d)



(e)



(f)

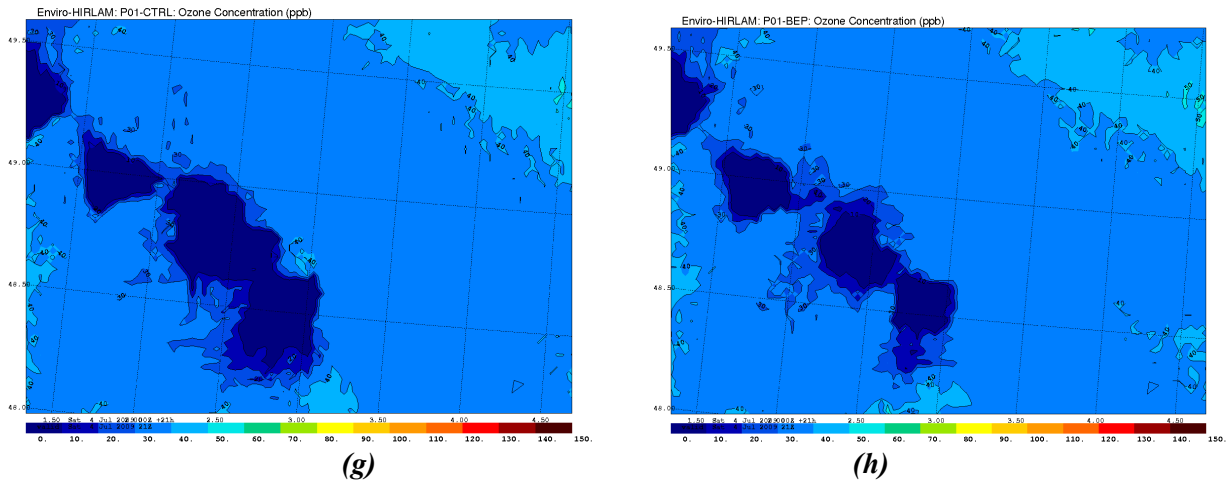


Figure 3.7.1: Variability of the ozone concentration (ppb) on a diurnal cycle – for the control (left column – a-c-e-g) vs. urbanized (right column – b-d-f-h) Enviro-HIRLAM-P01 model runs at (ab) 03, (cd) 09, (ef) 15, and (gh) 21 UTCs on 4 Jul 2009.

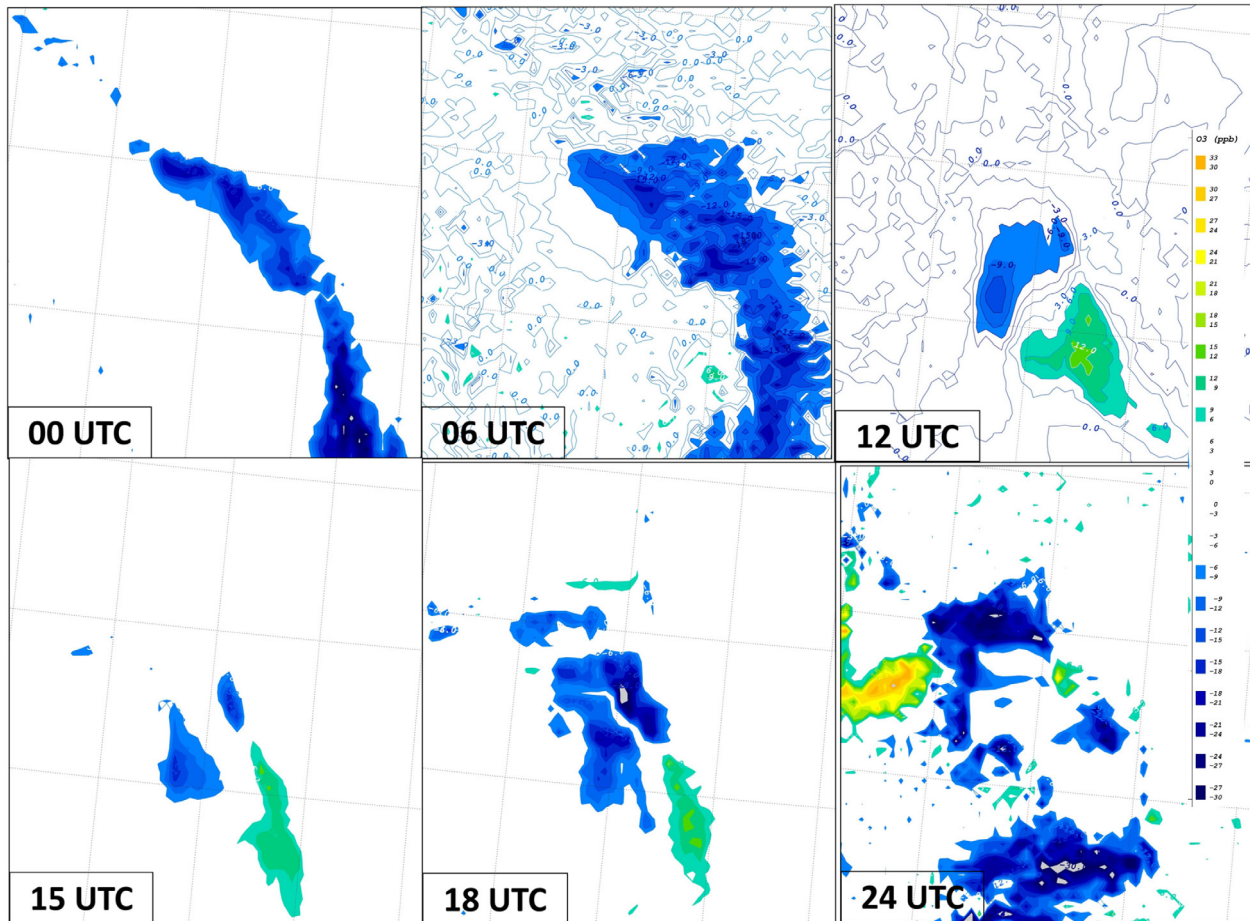


Figure 3.7.2: Paris metropolitan area: diurnal cycle variability of the difference fields (Enviro-HIRLAM-P01: control vs. urban runs) for the ozone concentration (in ppb) on 4 Jul 2009 (from 00 till 24 UTCs).

As seen in Figure 3.7.2, the differences between the runs are well seen on a diurnal cycle. At 00-06 UTCs, the ozone concentration is higher (by up to 15 ppb) for the urban run than for the control run, and this difference is observed to the east of the metropolitan area, which might be due to difference in wind speed following dominating wind direction. During 09-12-15 UTCs, there are both signs positive and negative differences between the runs. For the central areas of the Paris metropolitan

area the urban runs showed on average higher (by 6-15 ppb) ozone concentrations, but for the southern areas – the lower (by 6-12 ppb) ozone concentrations. This change is deepening for evening hours (18-21-24 UTCs) reaching a difference in concentration of up to ± 30 ppb with shifting these difference outside the boundaries of the metropolitan area.

The altitudinal (vertical) variability of the differences in ozone concentrations between two model runs at nighttime (00 UTC) is shown in Figure 3.7.3 at several model levels - 40, 39, 38, 37, 36, 35, 32, and 29 – distributed within the atmospheric boundary layer and corresponding to approximate heights of 31, 97, 176, 268, 372, 491, 952, and 1592 m above sea level. As seen, at two lowest levels (e.g. below 100 m) the spatial distribution of differences is similar to changes observed at night -early morning hours in Figure 3.7.2. At higher elevations starting from about 180 m, the control run shows higher concentrations compared with the urban run, and this difference is up to 30+ ppb with area expanding southerly of Paris. These differences started to diminish at about 1 km (model level - 32), and almost disappear at 1.6 km altitude. Modelling results showed that there are substantial differences observed not only in formation of meteorological parameters (shown in previous sections), but also in formation of chemical patterns, when the urbanization effects are included into the meteorological model.

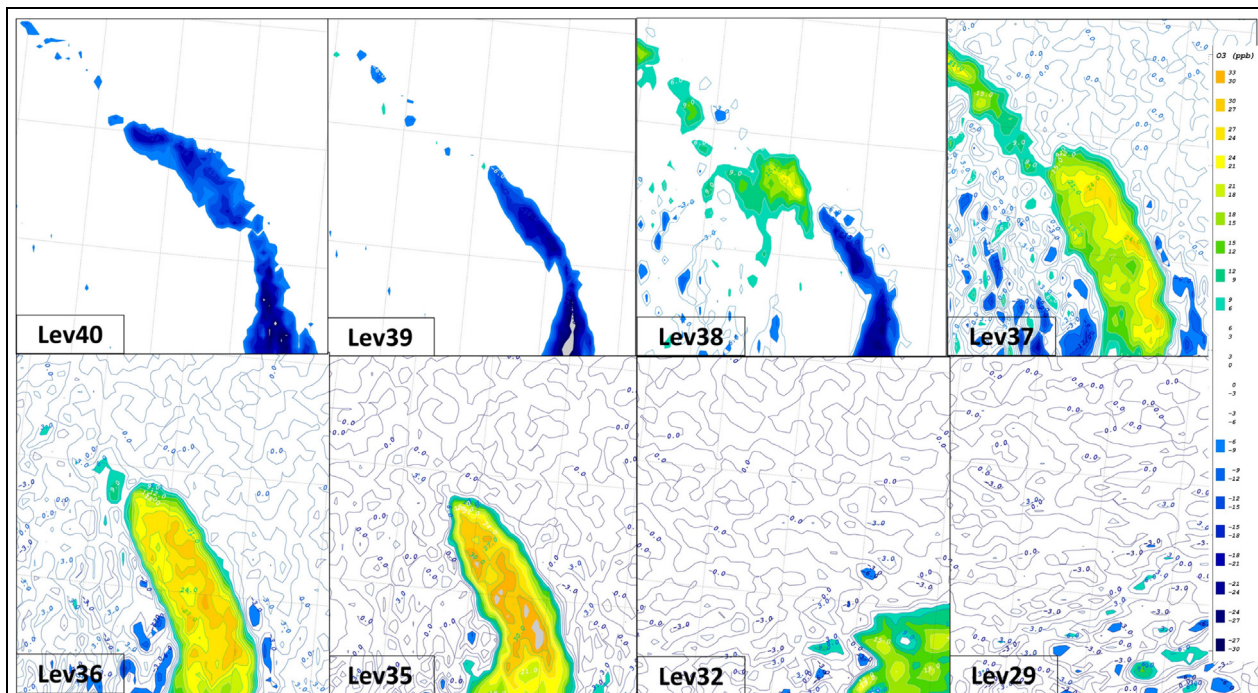


Figure 3.7.3: Paris metropolitan area: altitudinal variability of the difference fields (Enviro-HIRLAM-P01: control vs. urban runs) for the ozone concentration (in ppb) on 4 Jul 2009, 00 UTC.

4. Conclusions

In this pilot study, the influence of the Paris Metropolitan Area (PMA, France) on formation and development of meteorological and chemical patterns fields was investigated. In particular, the downscaling approach (15-5-2.5 km horizontal resolution) with running of the Enviro-HIRLAM model over the three enclosed domains down to the PMA was applied. The model runs were performed in two modes: control vs. modified (with Building Effect Parameterization, BEP module and varying Anthropogenic Heat Flux, AHF included) runs. As the Enviro-HIRLAM model is the on-line integrated meteorology-chemistry/aerosols system, the modelling of meteorological and chemical fields were done at the same temporal and spatial steps. In this study, the periods of the MEGAPOLI Paris Measurement Campaign were considered. The generated fields were evaluated for changes in meteorological (air temperature and relative humidity at 2 m, surface temperature, cloud cover, wind speed at 10 m, and boundary layer height) and chemical (on example of ozone) patterns on a diurnal cycle due to inclusion of urban effects into the model.

It was shown that in specific meteorological situations the urban effects can be of considerable importance over the large metropolitan areas such as Paris. These changes were identified for both meteorological parameters as well as for concentration of chemical species for specific dates as well as within the studied periods. The modification of model's land-surface scheme with including urban effects does not substantially (less than 3%) increase the computational time compared with the control run, as note that calculations are done only in urban grid-cells of the urban scale domain. This makes such modifications suitable for purposes of operational high resolution numerical weather prediction. Although the meteorological forecast is of key importance for the weather modelling community, but simultaneous generation of chemical forecasts (as "by-products" in this case) provides opportunities for delivering new products for the customers as well as strengthening collaboration with the air quality community (which still is applying the off-line approach for the atmospheric chemical transport modelling, ACTM using meteorological 3D fields at selected times, for example, every 1-3 hour time intervals).

The approaches applied as well as results obtained in this study will be used for reporting on the Deliverables (i.e. science reporting) of the FP7 EU MEGAPOLI project (<http://megapoli.info>) as well as for lecturing material and practical exercises (i.e. so-called small-scale research projects) for the YSSS-2011 on "*Integrated Modelling of Meteorological and Chemical Transport Processes / Impact of Chemical Weather on Numerical Weather Prediction and Climate Modelling*" (to be held in Jul 2011, Odessa, Ukraine; see more details at: <http://www.ysss.osenu.org.ua>). In particular, it will be used in practical exercises - URBAN "*The Influence of Metropolitan Areas on Meteorology*", COASTAL "*Coastal Effects (&Cities) Effects on Meteorology*", and AEROSOLE "*The Impact of Aerosols Effects on Meteorology*" (<http://www.ysss.osenu.org.ua/en/school-materials/exercises/exercises>).

Acknowledgments

The research leading to these results has received funding from the European Union's Seventh Framework Programme FP/2007-2011 under grant agreement n°218793.

The authors are thankful to Bent H. Sass (from DMI) for administrative support. Especial thanks to DMI IT Department for advice and computing support.

Authors are thankful to the MEGAPOLI Collaborator Dr. Alberto Martilli for providing BEP module for implementation into the Enviro-HIRLAM model, for constructive discussions and comments.

References

- Allen L., S Beevers, F Lindberg, Mario Iamarino, N Kitiwiroon, CSB Grimmond (2010): Global to City Scale Urban Anthropogenic Heat Flux: Model and Variability. Deliverable 1.4, MEGAPOLI Scientific Report 10-01, MEGAPOLI-04-REP-2010-03, 87p, ISBN: 978-87-992924-4-8; http://megapoli.dmi.dk/publ/MEGAPOLI_sr10-01.pdf
- Arnfield, A. J., Grimmond, C. S. B.: **1998**, 'An urban canyon energy budget model and its application to urban storage heat flux modelling', *Energy and Buildings*, 27, 61-68.
- Baklanov A., U. Korsholm, A. Mahura, C. Petersen, A. Gross, **2008**: ENVIRO-HIRLAM: on-line coupled modelling of urban meteorology and air pollution. *Advances in Science and Research*, 2, 41-46
- Bottema, M. (**1997**): Urban roughness modelling in relation to pollutant dispersion, *Atmos. Environ.*, 31, 3059-3075, 1997
- Chenevez, J., Baklanov, A. and Sorensen, J. H., **2004**: Pollutant transport scheme s integrated in a numerical weather prediction model: model description and verification results. *Meteorological Applications*, 11, 265-275.
- Clarke, J. A.: **1985**: Energy simulation in building design, Adam Hilger, Bristol
- Dupont, S. : **2001**, Modélisation dynamique et thermodynamique de la canopée urbaine : réalisation du modèle de sols urbains pour SUBMESO, *Doctoral thesis*, Université de Nantes, France.
- Dupont, S., Mestayer, P. (**2006**): Parameterization of the urban energy budget with the submesoscale soil model. *Journal of Applied Meteorology and Climatology*, 45 (12), 1744-1765.
- Dupont, S., Mestayer, P. G., Guilloteau, E., Berthier, E., and Andrieu, H. (**2006**): Parameterisation of the Urban Water Budget with the Submesoscale Soil Model (SM2-U), *J. Appl. Meteorol. Climatol.*, 45, 624-648, 2006
- Grimmond, C. S. B., and Oke, T. R.: **1999**, 'Heat Storage in Urban Areas: Local-Scale Observations and Evaluation of a Simple Model', *J. Appl. Meteorol.* **38**, 922-940.
- Gross, A., and A. Baklanov, **2004**: "Modelling the influence of dimethyl sulphide on the aerosol production in the marine boundary layer", *International Journal of Environment and Pollution*, 22(1/2): 51-71.
- Korsholm U.S. (**2009**): Integrated modeling of aerosol indirect effects. PhD thesis <http://www.dmi.dk/dmi/sr09-01.pdf>
- Korsholm U.S., A. Baklanov, A. Gross, A. Mahura, B.H. Sass and E. Kaas, (**2008**): Online coupled chemical weather forecasting based on HIRLAM – overview and prospective of Enviro-HIRLAM. HIRLAM Newsletter, 54: 1-17.
- Louis, J. F.: **1979**, 'A parametric model of vertical eddies fluxes in the atmosphere', *Boundary-Layer Meteorol.*, 17, 187-202
- Mahura A., Leroyer, S., Mestayer, P., Calmet, I., Dupont, S., Long, N., Baklanov, A., Petersen, C., Sattler, K., and Nielsen, N. W. (**2005a**): Large eddy simulation of urban features for Copenhagen metropolitan area, *Atmos. Chem. Phys. Discuss.*, 5, 11183-11213, doi:10.5194/acpd-5-11183-2005, 2005.
- Mahura A., Petersen C., Baklanov A., B. Amstrup, U.S. Korsholm, K. Sattler (**2008**): Verification of long-term DMI-HIRLAM NWP model runs using urbanization and building effect parameterization modules. HIRLAM Newsletter, 53: 50-60.
- Mahura A., Sattler K., Petersen C., Amstrup B., Baklanov A., **2005b**: DMI-HIRLAM Modelling with High Resolution Setup and Simulations for Areas of Denmark. *DMI Technical Report 05-12*, 45 p.



- Mahura, A., Baklanov, A., Petersen, C., Sattler, K., Amstrup, B., and Nielsen, N. W. (2006): ISBA Scheme Performance in High Resolution Modelling for Low Winds Conditions, *HIRLAM Newsletter*, 49, 22–35, 2006.
- Mahura, A., P. G. Mestayer, S. Dupont, I. Calmet, A. Baklanov, S. Leroyer, and N. Long, 2004: Comparison of short and long-term modelled latent, sensible, and storage heat fluxes employing numerical weather prediction model with and without urbanized modules. *Proc. Fourth Annual Meeting of the European Meteorological Society, Vol. 1, Nice, France, European Meteorological Society*, 391.
- Martilli, A., Clappier, A., Rotach, M. W., 2002: An Urban Surface Exchange Parameterisation for Mesoscale Models, *Boundary Layer Meteorology* 104, 261–304.
- Mestayer, P., S. Dupont, I. Calmet, S. Leroyer, A. Mahura, T. Penelon, 2004 : SM2-U : Soil Model for Sub-Meso scales Urbalized version. Model Description. Deliverable D4.2 for FUMAPEX WP4, Project report, Spring 2004, Nantes, ECN, France.
- Sass, B.H.; Nielsen, N.W.; Jørgensen, J.U.; Amstrup, B.; Kmit, M.; Mogensen, K.S., 2002: “The Operational DMI-HIRLAM System -2002-version”, *DMI Tech. Rep.*, 99-21.
- Schayes, G., Thunis, P. and Bornstein, R., 1996: Topographic Vorticity-Mode Mesoscale-K(TVM) Model. Part1: Formulation, *Journal of Applied Meteorology*, Vol. 35, pp. 1815-1824
- Unden, P., L. Rontu, H. Järvinen, P. Lynch, J. Calvo, G. Cats, J. Cuhart, K. Eerola, etc. 2002: HIRLAM-5 Scientific Documentation. December 2002, *HIRLAM-5 Project Report*, SMHI.
- Yang X., Petersen C., Amstrup B., Andersen B., Feddersen H., Kmit M., Korsholm U., Lindberg K., Mogensen K., Sass B., Sattler K., Nielsen W. 2005: The MDI-HIRLAM upgrade in June 2004. *DMI Technical Report*, 05-09, 35 p.

Appendix A1: Analysis of vertical sounding for Trappes station

MEGAPOLI Paris campaign measurement period (summer 2009): 1-31 Jul 2009

Month	Day	00 UTC			12 UTC		
		P (hPa)	WindCond	IS	P (hPa)	WindCond	IS
Jul	1	900-1000	LWC		800-1000	LWC	
Jul	2	900-1000	LWC		850-1000	LWC	
Jul	3	1000	LWC		900-1000	LWC	
Jul	4	900-1000	LWC		800-1000	LWC	
Jul	5	950-1000	LWC	640-680	1000	LWC	
Jul	6	1000	LWC		1000	LWC	
Jul	7	1000	LWC	650-700	1000	LWC	
Jul	8	1000	LWC		1000	LWC	675-700
Jul	9	1000	LWC		1000	LWC	
Jul	10	1000	LWC		925-1000	LWC	
Jul	11	900-1000	LWC	550-600	750-1000	LWC	
Jul	12	1000	TWC	470-550	1000	LWC	
Jul	13	1000	LWC		925-1000	LWC	
Jul	14	1000	LWC		1000	LWC	
Jul	15	1000	LWC		1000	LWC	
Jul	16	1000	LWC		1000	LWC	
Jul	17	1000	LWC	540-560	1000	LWC	
Jul	18	1000	LWC	600-725	1000	LWC	
Jul	19	1000	LWC	725	1000	LWC	
Jul	20	1000	LWC		1000	LWC	
Jul	21	1000	TWC		1000	LWC	
Jul	22	1000	LWC	500-575	1000	LWC	
Jul	23	1000	TWC		1000	LWC	
Jul	24	1000	LWC		1000	LWC	
Jul	25	1000	TWC		1000	TWC	
Jul	26	1000	LWC		1000	TWC	
Jul	27	1000	LWC		1000	LWC	
Jul	28	1000	LWC	725	900-1000	LWC	
Jul	29	1000	LWC		1000	LWC	
Jul	30	1000	LWC		1000	TWC	
Jul	31	1000	LWC		1000	LWC	

Comments to table:

LWC – low wind conditions (in main focus);

TWC – typical wind conditions;

HWC – high wind conditions;

P – pressure levels (in hPa);

IS – pressure level(s) at which the isothermal layer is presented and its vertical extension.

*MEGAPOLI Paris campaign measurement period (winter 2010): 15 Jan – 14 Feb 2010*

Month	Day	P (hPa)	WindCond	IS	P (hPa)	WindCond	IS
Jan	15	700-1000	LWC		900-1000	LWC	
Jan	16	1000	HWC		1000	TWC	
Jan	17	1000	LWC	700-780	1000	LWC	
Jan	18	700-1000	LWC		650-1000	LWC	
Jan	19	700-1000	LWC		1000	LWC	
Jan	20	1000	LWC		1000	LWC	
Jan	21	1000	LWC	750-800	1000	LWC	
Jan	22	1000	LWC	660-675	1000	LWC	
Jan	23	1000	TWC		1000	LWC	
Jan	24	900-1000	LWC		1000	LWC	
Jan	25	1000	LWC		500-1000	LWC	
Jan	26	600-1000	LWC		1000	LWC	
Jan	27	1000	LWC		1000	LWC	
Jan	28	1000	LWC	725-825	1000	LWC	800
Jan	29	1000	LWC	650-850	1000	LWC	
Jan	30	1000	LWC		1000	LWC	
Jan	31	1000	LWC		900-1000	LWC	
Feb	1	1000	LWC	825-850	1000	LWC	
Feb	2	1000	LWC		1000	TWC	
Feb	3	1000	LWC	625-725	1000	LWC	
Feb	4	1000	LWC	800	1000	LWC	
Feb	5	1000	LWC	600-800	1000	LWC	
Feb	6	1000	LWC		600-1000	LWC	
Feb	7	1000	LWC		900-1000	LWC	
Feb	8	500-1000	LWC	825-830	600-1000	LWC	825-830
Feb	9	1000	LWC	850-900	800-1000	LWC	
Feb	10	1000	LWC		1000	LWC	
Feb	11	1000	LWC	850-860	1000	LWC	850-900
Feb	12	1000	LWC	880-950	1000	LWC	
Feb	13	1000	LWC	720-800	1000	LWC	850-950
Feb	14	1000	LWC	850-900	900-1000	LWC	

Comments to table:

LWC – low wind conditions (in main focus);

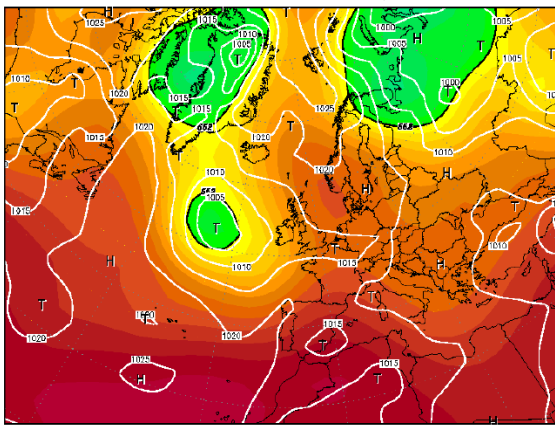
TWC – typical wind conditions;

HWC – high wind conditions;

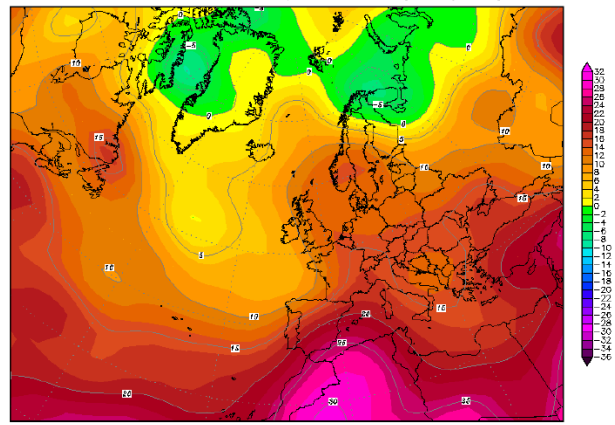
P – pressure levels (in hPa);

IS – pressure level(s) at which the isothermal layer is presented and its vertical extension.

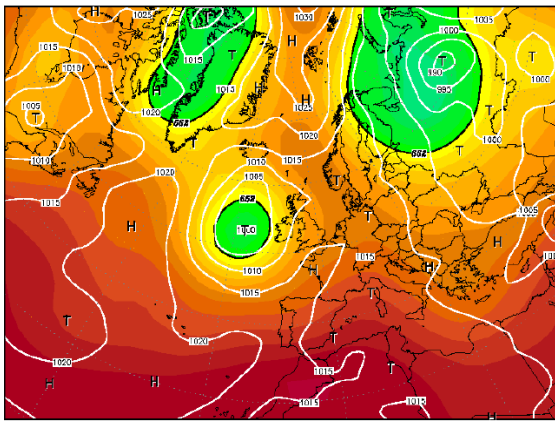
Appendix A2: Case study: 3-4 Jul 2009 – Meteorological situation



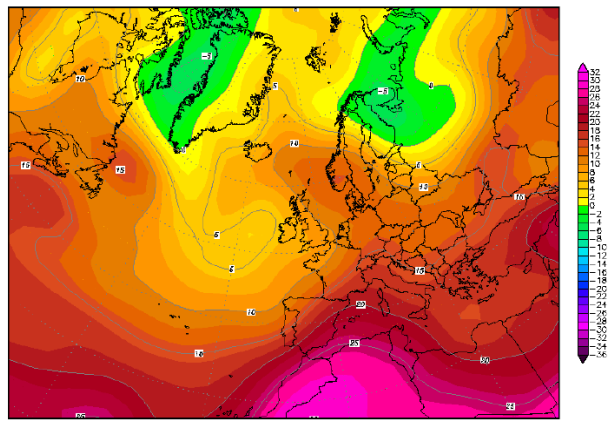
(a)



(b)



(c)



(d)

Figure: (ac) atmospheric pressure, hPa and (bd) air temperature, deg C at 850 hPa level on 3-4 Jul 2009 /source: link to web-site/.

Appendix A3: List of chemical species used in the chemical mechanism

Chemical species

N	Parameter	Molecular / Chemical Formula	Description	ID in grib-file
1	O3	O ₃	Ozone	99
2	NO2	NO ₂	Nitrogen dioxide	138
3	NO	NO	Nitrogen oxide	139
4	N2O5	N ₂ O ₅	Dinitrogen pentoxide	144
5	HNO3	HNO ₃	Nitric acid	145
6	H2O2	H ₂ O ₂	Hydrogen peroxide	146
7	SULF	H ₂ SO ₄	Sulfuric acid	147
8	CO	CO / C≡O	Carbon monoxide	148
9	HCHO	CH ₂ O / HCHO	Formaldehyde	149
10	ALD2	C ₂ H ₄ O / CH ₃ CHO	Acetaldehyde	150
11	C2H6	C ₂ H ₆ / H3C-CH3	Ethane	151
12	OLET	R-C=C	Terminal olefin carbon bond (R-C=C)	250
13	ETHE	C ₂ H ₄ / H ₂ C=CH ₂	Ethene /Ethylene/	153
14	ISOP	C ₅ H ₈ / CH ₂ =C(CH ₃)CH=CH ₂	Isoprene	154
15	TOLU	C ₇ H ₈ / C ₆ H ₅ -CH ₃	Toluene /Toluol/	155
16	CH3OOH	CH ₄ O ₂ / CH ₃ -OOH	Methyl hydrogen peroxide (MHP)	156
17	ROOH	R-OOH	Higher organic peroxide	157
18	MGLY	C ₃ H ₄ O ₂ / CH ₃ -CO-CH=O	Methylglyoxal	158
19	PAN	C ₂ H ₃ NO ₅ / CH ₃ COOONO ₂	Peroxyacyl nitrate	159
20	CRES	C ₇ H ₈ O /	Cresol & higher M.W. phenols (o-, m-, p-Cresol)	213
21	CRO		Methylphenoxy radical	214
22	XYL	C ₈ H ₁₀ , C ₆ H ₄ (CH ₃) ₂ , C ₆ H ₄ C ₂ H ₆	Xylene (o-, m-, p-Xylene)	215
23	ETHOOH		Ethyl hydrogen peroxide	216
24	DMS	(CH ₃) ₂ S / H ₃ C-S-CH ₃	Dimethyl sulphide /methylthiomethane/	217
25	XPAR		PAR removal operator	218
26	NH3	NH ₃	Ammonia	232
27	SO2	SO ₂ / O=S=O	Sulfur dioxide	233
28	OLEI		Internal olefin carbon bond (R-C=C-R)	234
29	OPEN		High molecular weight aromatic oxidation ring fragment	238
30	PAR		Paraffin carbon bond (C-C)	239
31	AONE	C ₃ H ₆ O / (CH ₃) ₂ CO	Acetone	243
32	ONIT	RNO ₃	Organic nitrate	244
33	CH3OH	CH ₄ O / CH ₃ -OH	Methanol	248
34	HCOOH	CH ₂ O ₂ / HCO-OH	Formic acid	249